CHAL-0169

COPY / OF 10

Marquardt AIRCRAFT CO.

SECRET

REPORT NO. 25,015

COPY NO. ______

SECRET marquardt CONTROL
Register No. 2079
Control Center B
Register Copy No. B10

REPORT NO. 25,015

(UNCLASSIFIED TITLE)

LOW PRESSURE COMBUSTION INVESTIGATION

BY: H. G. KRULL

14 JULY 1959

SECRET

CHAM-0168

COPY 1 OF 10

Marquardt AIRCRAFT CO.

SECRET

REPORT NO. 25,015

COPY NO. ______

SECRET CONTROL
marquardt
Register No. 2079
Control Center B
Register Copy No. B10

REPORT NO. 25,015

(UNCLASSIFIED TITLE)

LOW PRESSURE COMBUSTION INVESTIGATION

BY:

25X1

14 JULY 1959

SECRET

8a

Declassified in Part - Sanitized Copy Approved for Release 2012/08/14 : CIA-RDP89B00487R000400750006-4

NOTICES

This document contains information affecting the National Defense of the United States within the meaning of the espionage laws, Title 18, U.S.C. Sections 793 and 794. Its transmission or the revelation of its contents in any manner to an unauthorized person is prohibited by law.

- - - - - - - - - -

This document contains information proprietary to The Marquardt Corporation. It may not be reproduced, published, or distributed in any form, in whole or in part, without the authorization of The Marquardt Corporation or the Procuring Agency.

Marquardt AIRCRAFT CO.

SECRET

REPORT NO. 25,015

(Unclassified Title)

LOW PRESSURE COMBUSTION INVESTIGATION

Contract No. NOas 59-0117

Marquardt Project No. 211

14 July 1959

PREPARED BY

APPROVED BY

25X1

ASTRO - A Division of
The Marquardt Corporation
Van Nuys, California

SECRET

Declassified in Part - Sanitized Copy Approved for Release 2012/08/14 : CIA-RDP89B00487R000400750006-4

CONTENTS

ILLUSTRATIONS

ILLUSTRATIONS (Continued)

SUMMARY

Combustor performance data were obtained for various fuels at combustor inlet conditions simulating Mach 2.3 to 3.0 in the region of 100,000 ft altitude. The following fuels were investigated: (1) SF-1, (2) HiCal-3, (3) pentaborane, (4) vaporized hexane, and (5) liquid hexane.

Insofar as combustion performance is concerned, the boron hydride fuels (pentaborane and HiCal-3) operated over a wide range and ignited with ease, indicating exceptional burning stability. These fuels were so stable at the low pressure conditions that lean blowout could not be ascertained. SF-1 demonstrated smooth burning characteristics with a lean blowout limit at an equivalence ratio of approximately 0.17 at a combustor pressure slightly less than 3.0 psia. SF-1 fuel did not light as easily as the boron hydrides. Vaporized hexane burned smoothly and was superior to liquid hexane but did not burn as lean or ignite as easily as the boron hydrides or SF-1 fuels. Pentaborane had a combustion efficiency of approximately 100 percent at an equivalence ratio of 0.16, while the combustion efficiency of HiCal-3 was lower, with a value of 86 percent at an equivalence ratio of 0.136. The combustion efficiency of SF-1 fuel was nearly constant at approximately 88 percent over a range of equivalence ratios from 0.178 to 0.387. The combustion efficiency of vaporized hexane was above 95 percent for equivalence ratios from 0.47 to 0.69. The performance of liquid hexane was very sensitive to burner pressure, requiring higher pressure or higher equivalence ratios to obtain the combustion efficiencies obtained with vaporized hexane.

The nonmetallic tailpipe was operated a total time of 2-1/2 hrs. Tailpipe skin temperatures ranging from 800°F to 1150°F were obtained during this period. The tailpipe was still serviceable after the test, only showing signs of partial delamination on the inner surface of the combustion chamber. There was no evidence of deterioration externally.

The lowest infrared emittance was obtained with SF-1 fuel. The next lowest was HiCal-3 and hexane was the highest. The total infrared emittance of the boron hydride fuel was less than one third that of the hydrocarbon fuel.

The results of this investigation have shown that the required high performance at the conditions of interest (low pressure and lean fuel-air ratio) is obtainable with various fuels, and that a nonmetallic tailpipe is suitable for operation at these conditions.

Declassified in Part - Sanitized Copy Approved for Release 2012/08/14 : CIA-RDP89B00487R000400750006-4

I. INTRODUCTION

In early 1958, Commander A. D. Struble, U.S.N. Bureau of Aeronautics, contacted The Marquardt Corporation to discuss the feasibility of a Mach 3.0 ramjet engine, for a cruise vehicle, having the following special features:

(1) Operating Altitude

Extremely high altitude (200,000 ft), which is far beyond the limits of existing state-of-the-art.

(2) Materials

Plastic materials to be used throughout the engine except for limited areas near the center of the engine.

(3) Size

The engine size required is three or four times as large as current state-of-the-art engines.

A study was initiated immediately to evaluate the problem. The conclusions of this work indicated that a lightweight, nonmetallic ramjet engine was feasible and that combustion probably could be maintained under the assigned conditions. However, combustion was still a big unknown factor, because no actual data existed for conditions simulating Mach 3.0 and 200,000 ft altitude (i.e., burner pressure $\approx$ 0.1 psia and burner inlet temperature $\approx$ 800°F).

In May 1958, under BuAer sponsorship (Contract NOas 58-813), The Marquardt Corporation initiated a three month experimental program to establish the feasibility of maintaining combustion down to a pressure level of 0.1 psia, utilizing pentaborane fuel. The results of these tests were very encouraging and showed that pentaborane could be burned at pressures at low as 0.054 psia. No attempt was made to determine combustion efficiencies.

Concurrent with the above work, Marquardt transmitted engine data to CONVAIR, San Diego, California and Goodyear Aircraft Corporation, Akron, Ohio. As a result of this interchange and the success of the experimental combustion program, BuAer sponsored a detailed preliminary design study of a ramjet engine that would cruise at 150,000 ft altitude, and a Mach number of 3.0, with a range of 3,000 nautical miles. (The reduction in altitude resulted from studies of CONVAIR and Goodyear which showed flight vehicle limitations.

The ramjet engine preliminary design study was a team effort involving Marquardt, CONVAIR, and Goodyear. Marquardt performed the engine design and performance studies, CONVAIR performed the over-all system studies, and Goodyear performed the air frame and engine structural feasibility studies. The engine preliminary design studies, plus the other above-mentioned studies, are all presented in Reference 1.

Due to the encouraging results on the preliminary design studies and the feasibility combustion studies, the presently reported experimental program was initiated under Navy Contract NOas 59-0117 to verify some of the assumptions used in the previous analysis. The objectives of this program were as follows:

(1) to evaluate combustion performance of a 28-inch ramjet engine at low combustion pressures and lean fuel-air ratios using pentaborane, HiCal-3, SF-1, and hydrocarbon fuels

(2) to evaluate the structural durability of a nonmetallic tailpipe and exhaust nozzle

(3) to determine the infrared emission of the combustion gases

The experimental work for this program was directed toward high combustion efficiency of the above-mentioned fuels at minimum obtainable combustion pressures and in the lean fuel-air ratio range corresponding to exhaust gas temperatures of approximately 2000°F. The tests were conducted at combustor inlet conditions simulating the maximum obtainable altitude in the AF-MJL Cell 8 facility in the region of Mach 3.0 flight.

The experimental investigation was conducted on an exploratory basis without regard for combustor or engine optimization. Neither the budget or available test time permitted modifications other than test expedients to be made to the basic combustor configuration.

Combustor performance data, including combustion efficiency and combustor pressure drop, were obtained at simulated flight Mach numbers in the region of 2.5 to 3.0 and 100,000 ft altitude for pentaborane, SF-1, HiCal-3, liquid hexane, and vaporized hexane. Endurance runs were conducted on the nonmetallic tailpipe and time history plots of tailpipe skin temperature and exhaust gas temperature were obtained. Infrared spectral radiant emission of the exhaust products of all fuels except pentaborane were obtained over a wavelength band from 1.5 to 7 microns. The results of the experimental investigation are reported in the following sections of this report.

II. EXPERIMENTAL SETUP

A 28-inch diameter heavy duty, direct-connect engine was utilized for the experimental investigation. A photograph of the engine installed in the AF-MJL Cell 8 test facility is shown in Figure 1, and a schematic drawing of the engine is shown in Figure 2. A round hole grid (flow straightener) with approximately 38 percent blockage was installed a short distance upstream of the flame holders, as shown in Figure 2.

The basic flame holder configuration was a 16 element spoke configuration with the gutters swept back 30°, as shown schematically in Figure 3. The flame holder configuration was so arranged that the gutters were interchangeable, also shown in Figure 3. Two different gutter elements were used during the investigation. A short ceramic-coated gutter, Figure 4, giving 72 percent projected blockage, was used for the special fuels. The ceramic coating, which was applied to the surfaces exposed to the flame, provided a glowing flame stabilizing surface. An extended, uncoated gutter was used for the hydrocarbon fuel, as shown in Figure 5. The effective blockage of both gutter configurations was the same.

Fuel was injected into the high velocity region between the spokes, as illustrated in Figure 3. Cross-stream injection was utilized with the sprays directed slightly downstream. Eighty injection points were provided and the fuel nozzles were encased within the spokes. The number of injection points actually utilized during each phase of the program varied and will be discussed under the Results Section of this report. The fuel nozzles that were used during the tests varied between the fuels and included the following: (1) 0.011-inch diameter orifice flat spray nozzles, (2) 0.020-inch diameter orifice flat spray nozzles which were modified from 0.011-inch diameter nozzles, and (3) 0.060-inch diameter fixed orifice nozzles for gaseous fuels. The fuel nozzle employed for each fuel is discussed along with each fuel tested under the Results Section of this report. In the design of the flame holder and fuel injector unit, purge air was provided around the fuel nozzles to help wash the special fuels deposition from the nozzle face. This purge air was supplied from an external source and was also used to cool the fuel manifold.

Combustion chamber lengths of 27 inches, 60 inches, and 126 inches were used during the investigation. The combustion chamber length is defined as the distance between the downstream edge of the flame holder to the exhaust nozzle inlet. For the combustor evaluation tests, a metallic tailpipe was used as shown in Figure 1. The nonmetallic tailpipe, which was investigated for structural durability, is shown in Figure 6.

The nonmetallic tailpipe was fabricated by Goodyear Aircraft Corporation, Akron, Ohio and measured 6 ft long and 28 in. in diameter. Both the metallic and nonmetallic tailpipes had an exhaust nozzle throat to combustion chamber area ratio of 0.25. The metallic tailpipes were equipped with convergent-divergent exhaust nozzles to increase the pressure range over which the exhaust nozzle could be choked.

A hydrogen-spark igniter was used for igniting the nonpyrophoric fuels.

III. INSTRUMENTATION

Engine Instrumentation

A listing of the pressure and temperature instrumentation used throughout the engine is given in Table I and is shown schematically in Figure 2. Presented also in Table I are the types of measuring instruments and the reading accuracy. Thermocouples were provided to document the combustion chamber wall temperatures of the nonmetallic tailpipe during the structural reliability tests. Two of these thermocouples, T_{W_2} and T_{W_3}, were laminated into the wall at approximately the center of the wall material and the third, T_{W_1}, was attached to the external wall surface.

Since both gaseous and liquid fuels were tested, two independent fuel metering systems were required. For the gaseous fuels, a choked venturi was used and for the liquid fuels a vane-type flow meter was employed.

Infrared Measurement Instrumentation

Infrared instrumentation was installed to measure the infrared spectral radiant emittance of the exhaust gases. The major instrument was a Beckman Model IR-2 Infrared Spectrometer. This instrument is divided into four units. The main unit consisted of the optical system, the wavelength selective unit, and the detector. The second and third units are the power supply and amplifier, and the fourth unit is an x-y strip chart recorder. The main unit was modified for use with an external infrared source, and a wavelength drive unit was also installed which permitted the wavelength spectrum to be swept through 1 to 15 microns.

In Figure 7 is shown the installation of the infrared spectrometer and associated equipment. The approximate distance from the spectrometer aperture to the axis of the jet was 105 inches. In order to minimize infrared transmission losses, the exhaust gases were viewed through a 4-1/2 in. hole in a plate which was used to replace the glass window.

The infrared spectrometer had previously been calibrated against a laboratory-type black body furnace source. Prior to using the instrument for this program the earlier calibration was rechecked with a commerical Barnes Engineering Co. standard black body source and was found to be sufficient for the purposes of this investigation.

IV. RESULTS

Combustor Performance

The results of the experimental program showed that high combustion efficiencies were obtained for all fuels tested at simulated combustor inlet conditions corresponding to flight Mach numbers from 2.3 to 3.0 and an altitude of approximately 100,000 ft. In general, the pentaborane and HiCal-3 fuels operated over a wide range and ignited with ease, indicating exceptional burning stability. SF-1 burned smoothly but did not ignite as easily as the boron-base fuels. The hydrocarbon fuel burned smoothly but did not burn as lean or ignite as readily as the other fuels. A summary of the combustion performance of the fuels tested is presented in Figure 8. A summary of the details of each configuration and the test conditions of each run is presented in Table II. Detailed results of the combustor performance that were obtained with the various fuels are presented in the following sections of this report, and the methods used for data reduction are presented in Appendix A.

SF-1 Fuel -- The configuration used for evaluating the combustor performance with SF-1 fuel utilized all 80 injection orifices (0.060-inch diameter) and the short ceramic-coated gutters. Tailpipe lengths of 27 inches (Run 4) and 60 inches (Run 5) were investigated.

The combustor performance that was obtained with both tailpipe lengths is presented in Figure 9. Combustion efficiency, combustor pressure, and combustor pressure recovery are plotted against equivalence ratio. Combustion efficiency was nearly constant over the range of equivalence ratios tested, varying only between 87 and 90 percent. Combustor length had no effect on combustion efficiency or combustor pressure recovery for the lengths tested. Combustion was smooth all the way down to lean blowout, which occurred at an equivalence ratio of 0.171. Ignition attempts were unsuccessful with the exit choked; however, ignition was obtained with an unchoked exhaust nozzle at pressures below 6 psia.

HiCal-3 Fuel -- The same burner configuration was used for HiCal-3 fuel as was used for SF-1 fuel except that the 0.060-in. diameter fuel orifices were replaced with 0.011-in. diameter orifices. Combustor lengths of 60 inches (Run 2) and 126 inches (Run 3) were investigated, and the results are shown in Figure 10. The combustor operation with HiCal-3 fuel was very smooth and extremely stable. No lean blowout could be ascertained during choked nozzle operation. Incipient clogging of the fuel manifold and injectors was experienced. However, some representative data were obtained with unclogged fuel system with combustion efficiency ranging from 83 to 96 percent at an equivalence ratio of approximately 0.140. The data obtained with the unclogged fuel system are shown on Figure 10 by the open symbols and the data obtained with the partially clogged fuel system are shown by the solid symbols. As would be expected, the combustion efficiency was somewhat lower with the fuel system partially clogged as a result of poor fuel distribution. It is felt that the plugging problem was a result of the manifold becoming overheated by the combustor inlet air. Apparently, the cooling air that was supplied from an external source for cooling the manifold was not sufficient to keep it below the decomposition temperature of the fuel.

This was partly substantiated by the fact that for Run 3, where the manifold was partially clogged for the complete run, the fuel temperature in the manifold at the beginning of the run was 150°F and for Run 2, which only had clogging problems near the end of the run, the initial fuel temperature in the manifold was 70°F. Since bulk fuel temperatures of 150°F were measured, this means that the fuel temperature near the walls of the manifold could have been well above the decomposition temperature of the fuel (250°F) at the beginning of Run 3 resulting in fuel decomposition and fuel system plugging.

No attempt was made to remedy the plugging problem during this investigation; however, it is felt that decomposition of the fuel could be prevented by either proper hardware design (to prevent overheating) or by using a more stable boron hydride fuel. For example, the decomposition temperature of HiCal-4 and HiCal-5 fuels is 350°F and 800°F, respectively, as compared to 250°F for HiCal-3 fuel.

<u>Pentaborane Fuel</u> -- Two documentation runs (1 and 10) were conducted with pentaborane fuel and only the last run (10) yielded usable data. The burner configuration used for the first run was exactly the same as the configuration used for HiCal-3 fuel. A combustor length of 60 inches was used. Immediate clogging of the fuel system occurred, which necessitated shutdown after only approximately 30 seconds burning time. The engine ignited very easily with a choked exhaust nozzle at approximately 3 psia combustor pressure. Postrun inspection of the engine showed heavy yellow deposits completely clogging the filters and fuel manifold, as shown in Figures 11 and 12. Subsequent investigation revealed that the fuel received from the vendor contained excessive amounts of decomposed solids, which probably contributed to the peculiar abruptness of the clogging. It is believed that the decomposition of the pentaborane was caused by contaminated shipping cylinders.

In order to reduce chances of clogging during the next run, the fuel was filtered prior to filling the run tank and the 0.011-in. diameter orifices were replaced with 0.020-in. diameter orifices. Since larger orifices were used, the number of injection points was reduced to 64 by blocking off the outboard nozzles. With this configuration, the combustion characteristics were similar to HiCal-3 fuel in that burning was very smooth and stable, and a lean blowout could not be ascertained. Shortly after ignition there was evidence of the fuel system starting to clog. The fuel system started to clog slowly at first, but progressed rapidly during the latter part of the run. The data that were obtained prior to clogging is shown in Figure 13. The data that were obtained after extensive clogging had occurred was unrepresentative and was, therefore, rejected. The data that were obtained before clogging occurred show that combustion efficiencies ranging from 85 to 100 percent were obtained at equivalence ratios between 0.156 and 0.178. The clogging of the fuel system after the run had started was probably a result of overheating the fuel in the manifold, as also occurred with HiCal-3. Here again, this problem could be eliminated either by improved design or by use of more stable HEF fuels, such as HEF-3 or HEF-4.

After the run had been completed, it was discovered that the pentaborane had been inadvertently contaminated with toluene during fuel transfer operations. Two samples were taken from the run tank, one from the dip tube and the other from the bottom of the tank. An analysis of the samples showed 17 percent toluene in the dip tube sample and 10 percent toluene in the bottom tank sample. The combustion efficiency calculations are based on noncontaminated pentaborane; the effect of contamination is approximately 2-3 percentage points in combustion efficiency.

Vaporized Hexane -- The burner configuration for the vaporized hexane consisted of 64 fuel nozzles of 0.060-in. diameter (outboard nozzles blocked off in each spoke), the extended gutters, and a 60-in. tailpipe length. Because of the lower reactivity of the hydrocarbon fuel, the longer gutters were used to increase the volume of the recirculation zone and, hence, increase the burner stability.

The combustor performance that was obtained with vaporized hexane (Run 8) for three mass flow conditions is shown in Figure 14. Burning appeared very smooth and stable over the operating range of the burner. Lean blowout occurred at an equivalence ratio of approximately 0.38 for all conditions, which was considerably higher than for the boron hydride and SF-1 fuels. Maximum combustion efficiencies ranging between 96 to 98 percent were obtained at equivalence ratios ranging from 0.475 to 0.68.

Liquid Hexane -- For investigating the liquid hydrocarbon-type fuels, hexane was chosen, which is in the same family as JP-4 fuel. In order to test liquid hexane without jeopardizing the remaining test schedule, it was necessary to compromise the fuel injection configuration. The same configuration was used that was used for the vaporized hexane except that the fuel manifolds in every other spoke were blocked off, making a total of 32 injection points. Even with the large reduction in injection points, the fuel nozzles still operated at very low pressure differentials at the low fuel flows tested. The combustor performance that was obtained with liquid hexane (Run 9) is shown in Figure 15. Combustion did not appear to be as smooth and steady as it was for the other fuels, as evidenced by the low frequency pressure oscillations (1-2 cps); however, a maximum combustion efficiency of 98 percent was obtained at a burner pressure of approximately 8 psia. Combustion performance was very sensitive to pressure, as evidenced by a drop off in combustion efficiency to 75 percent at a pressure of 3 psia. The combustion efficiency obtained with the liquid hexane was somewhat lower than those obtained with vaporized hexane for a given burner pressure. The lean blowout limit for liquid hexane also occurred at a considerably higher equivalence ratio than for vaporized hexane. The lean stability limits were also very sensitive to burner pressure, as shown in Figure 15. Considering the makeshift burner configuration, relatively good performance was obtained with the liquid hexane.

Nonmetallic Tailpipe Structural Durability Tests

Two endurance tests were made (Runs 6 and 7) totalling 2-1/2 hrs burning time. The object of these tests was to evaluate the structural durability of the nonmetallic tailpipe under conditions of simulated wall temperatures and pressure differential across the combustor wall. SF-1 fuel was used for this evaluation instead of the boron hydrides because of its low cost and availability. The same burner configuration was used that was used for the SF-1 combustor evaluation tests, except that the outboard fuel nozzle in each spoke was blocked off. A photograph of the nonmetallic tailpipe installed on the test engine is shown in Figure 16a. The first endurance run (Run 6) was terminated after approximately 10 minutes burning time due to a hot spot in the nonmetallic tailpipe, which was observed developing 10 inches downstream of the flame holder. Time history curves of the run are shown in Figure 17. A postrun inspection revealed that a missing insert in one of the outboard fuel nozzles was responsible for the localized hot spot. The hot spot resulted in localized damage to the tailpipe, as shown in Figure 16b. The conditions established for the endurance testing were chosen to yield material wall temperatures which are representative of an engine configuration which incorporates an inner metallic cooling liner in the combustion chamber, as illustrated in Figure B39 of Reference 1. In the case of a fuel nozzle failure in a flight engine, such as occurred during Run 6, the liner would protect the nonmetallic tailpipe from overheating.

Due to the damage that occurred, a 38-in. length of the nonmetallic tailpipe was removed and replaced with a metallic section, as shown in Figure 16c. The reworked tailpipe was operated (Run 7) for a period of 140 minutes. The time history curves of the run are shown in Figure 18. The first 105 minutes of the operation were at a maximum wall temperature of 820°F. In the last 35 minutes of the run, the wall temperature was increased so that by the time of fuel exhaustion the throat of the exhaust nozzle had operated up to a temperature of 1150°F. A postrun inspection of the tailpipe revealed that it was still serviceable. There were no visual indications of deterioration at the throat of the nozzle where the maximum temperature occurred. Some wear was evident on the inner surface of the combustion chamber, as evidenced by partial delamination as shown in Figure 19. Since pre-prototype models are usually of poor quality control, there may have been variations in the layers of material throughout the tailpipe which could have accounted for the partial delamination. There was no evidence of deterioration on the outer surface.

Infrared Emission Characteristics

Infrared radiation data were obtained for all fuels except pentaborane. Even though data were not obtained for pentaborane, the data that was obtained for HiCal-3 can be considered representative of the boron hydride fuels. The tests were originally set up to laterally scan the jet, but due to limited quantities of available fuel and the length of time required to complete a spectral scan, it was decided to omit the lateral scanning entirely and take a spectral scan only on the longitudinal centerline of the exhaust plume.

While the presence of moisture within the instrument, which would cause atmospheric absorption on the infrared radiation, was eliminated by continuously flushing the spectrophotometer with dry nitrogen gas, it is known that atmospheric attenuation was encountered due to moisture within the interior of the cell during the engine runs. It was impossible to correct the data for this attenuation because of the absence of information on the exact concentration of water vapor within the cell. Again, using the standardized nomenclature acceptable in infrared measurements, the measured quantities should be regarded as "apparent" rather than absolute.

The infrared data that were obtained are summarized in Figure 20. Infrared spectral radiant emittance ($watts/cm^2/micron$) is plotted against wavelength in microns for SF-1, HiCal, and hexane fuels. The total infrared emission for these fuels was obtained by integrating these curves over a wavelength band from 1.5 to 7 microns, and the value is also shown in Figure 20. It can be seen that the total emittance of a hydrocarbon fuel is over three times that of a boron hydride and ten times that of SF-1 fuel.

In examining the spectral radiant emittance curves for each fuel, it can be seen that hexane shows peaks in the vicinity of 2.8 to 4.4 microns, which is similar to data which has been previously reported on the measurements of the exhausts of jet aircraft engines burning hydrocarbon fuels. HiCal-3 shows two peaks at 2.8 and 4.4 microns and, in addition, a third peak was obtained around 5 microns. This third peak is reported to be typical of boron hydride fuels. In the case of SF-1 fuel, the three characteristic peaks were noted at 2.8, 4.4, and approximately 5.5 microns with a fourth peak beyond 6.5 microns. It can be seen from the results that each fuel type has its own characteristic spectral radiant emittance curve. It is also interesting to note that the maximum peak spectral radiant emittance for hexane is almost 5-1/2 times that of the boron hydride and 50 times that of SF-1 fuel.

V. CONCLUSIONS

The big questions in establishing the feasibility of the special ramjet of Reference 1 were the combustor performance and the durability of a nonmetallic tailpipe. The present investigation has looked into both of these questions, and the results have been very encouraging.

The combustor performance evaluation tests have shown that, for the conditions of interest (lean fuel-air ratios and burner pressures from 3 to 6 psia), high combustion efficiencies were obtained with all fuels tested. For the boron hydrides, SF-1, and the vaporized hexane, combustion was smooth and stable over the range of interest with the boron hydrides having the best lean stability limits. Since no attempt was made to optimize combustor geometry, it could be expected that even higher combustor performance could be obtained if additional work were undertaken to optimize the combustor.

Higher combustion efficiencies were obtained with pentaborane than were predicted for use in the preliminary engine design work of Reference 1. Curves of the predicted combustion efficiencies that were used for the preliminary design work are shown in Figure 21. An actual experimental data point that was obtained with pentaborane is plotted on the curve for comparative purposes. As shown by the figure, much higher combustion performance was obtained, using a shorter burner length, than had been predicted. As a result, it can be seen now that the earlier vehicle performance estimates were very conservative. Although problems in testing occurred, these are typical in all development programs. Hence, in a concentrated predevelopment evaluation, as performed, these results are extremely encouraging.

As to the question of the durability of the nonmetallic tailpipe, the tests have shown that such a tailpipe is suitable for high altitude operation for a combustion chamber using an inner metallic liner. The structural integrity of the nonmetallic tailpipe was demonstrated at wall temperatures ranging from approximately 800°F to 1150°F. In a flight application, the nonmetallic tailpipe temperatures were predicted (Reference 1) to be approximately 800°F. These results have shown that the concept of a nonmetallic ramjet, which must operate at extremely high altitudes and lean equivalence ratios, is feasible.

In addition, the results have also shown that the infrared radiatiom emittance for the boron hydride fuels, which showed the best combustion characteristics, is relatively low, being only about one third that of a hydrocarbon fuel.

APPENDIX A

DATA REDUCTION METHODS

Combustion efficiency is defined as the ratio of actual to ideal temperature rise. The double cold choke technique was used to calculate combustion efficiency (when the choke points were the air metering nozzle and the exhaust nozzle throat). The exhaust nozzle to air metering nozzle total pressure ratio under burning conditions, $(P_{t_4}/P_{t_o})_H$, divided by the same pressure ratio during cold flow conditions $(P_{t_4}/P_{t_o})_c$, can be expressed as

$$(P_{t_4}/P_{t_o})_H \Big/ (P_{t_4}/P_{t_o})_c = (1 + f/a)\sqrt{\frac{T_{t_o} + \eta_c \, \Delta T_i}{T_{t_o}}} \; \frac{\left(\frac{P}{P_t}\overset{\circ}{m}\right)^*_c}{\left(\frac{P}{P_t}\overset{\circ}{m}\right)^*_H}$$

where

η_c = combustion efficiency

ΔT_i = ideal temperature rise

$\left(\frac{P}{P_t}\overset{\circ}{m}\right)^*_c$ = sonic mass flow parameter for cold flow conditions

$\left(\frac{P}{P_t}\overset{\circ}{m}\right)^*_H$ = sonic mass flow parameter for exhaust nozzle hot flow conditions.

Combustion efficiency can then be expressed as

$$\eta_c = \frac{T_{t_o}\left\{\left[\dfrac{(P_{t_4}/P_{t_o})_H \left(\dfrac{P}{P_t}\overset{\circ}{m}\right)^*_H}{(P_{t_4}/P_{t_o})_c \left(\dfrac{P}{P_t}\overset{\circ}{m}\right)^*_c (1 + f/a)}\right]^2 - 1\right\}}{\Delta T_i}$$

The various assumptions that were made in reducing the performance data are outlined below for each fuel investigated.

1. Pentaborane

The ideal temperature rise used for pentaborane was taken from Reference 2 and is given in Figure 22. In the absence of reliably established values of the physical properties of the products of combustion, the simplifying assumption was made that the specific heat ratio γ was constant and equal to 1.286. It may also be assumed that the test data is within the range in which condensed products (B_2O_3) are present in the exhaust gases. Check calculations, using a limited amount of exact thermodynamic data which has recently been obtained, indicate that the combustion efficiencies that were calculated using the above assumptions were on the conservative side.

2. HiCal-3

The ideal temperature rise used for HiCal-3 was taken from Reference 3 for HEF-3 and the curve for an inlet temperature of 700°F was abstracted and is shown in Figure 23. The assumptions in regard to the specific heat ratios of the products of combustion were the same as for pentaborane.

3. SF-1

The ideal temperature rise characteristics were taken from Reference 4 and are shown in Figure 24. The mass flow function for the combustion products of SF-1 and air, at the adiabatic flame temperature, was derived using published specific heat values. No dissociation of the products of combustion was assumed. (Actually, the effect of dissociation is negligible below 3000°F exit temperature.) No allowance was made for influence of incomplete combustion on the exit mass flow parameter. Within the range of the experimental data, this factor was shown to cause less than 2 percent error in calculated efficiencies. The derived values of specific heat ratio, gas constant, and mass flow parameter, assuming complete combustion of SF-1 with standard air, are shown in Figure 25 as functions of fuel-air ratio.

4. n-Hexane

The ideal temperature rise for JP-4 fuel at 0.2 atm was used and is shown in Figure 23, having been obtained from Reference 3. The mass flow parameter of the products of combustion in the choked exhaust nozzle was calculated using published specific heat ratios for each component as for the SF-1 above. This method was used for fuel-air ratios up to 0.03, and above this value previously derived mass flow parameter vs. fuel-air ratio plots were utilized, taken from Reference 5. The same performance reduction curves were used for both the liquid and the vaporized hexane test data.

REFERENCES

1. Marquardt Aircraft Co. Report 25,004 (December 1958); Analytical and Experimental Studies of a Supersonic Ramjet for Flight at Very High Altitude. SECRET.

2. NACA RM E55A31 (June 1955); Analytical Evaluation of Effect of Inlet-Air Temperature and Combustion Pressure on Combustion Performance of Boron Slurries and Blends of Pentaborane in Octene-1, L. K. Tower. CONFIDENTIAL.

3. Marquardt Aircraft Co. unpublished memorandum (12 June 1957); Ideal Temperature Rise Curves for Triethyl Aluminum, Triethyl Boron, HEF-2 and JP-4 Fuels, D. J. Simkin. CONFIDENTIAL.

4. NACA RM E57D24 (26 February 1957); Survey of Hydrogen Combustion Properties, I. L. Drell and F. E. Belles. UNCLASSIFIED.

5. Marquardt Aircraft Co. unpublished memorandum (2 August 1957); Accuracy of Present Method of Calculating Combustion Efficiency, T. Rodgers. UNCLASSIFIED.

TABLE I

INSTRUMENTATION LIST

Parameter	Description	Recorder or Indicator	Reading Accuracy
P_o	Static pressure in facility ducting upstream of inlet nozzle	Differential H_g manometer, atmospheric reference	0.10" Hg
P_n	Metering nozzle throat static pressure		
P_{183}	Diffuser static pressure upstream of burner		
P_{1841} thru P_{1846}	Diffuser total pressure rake upstream of burner (6 probes)		
$P_{3.5}$ and $P_{3.8}$	Combustion chamber static pressure		
P_{4011} thru P_{4018}	Total pressure rake at combustion chamber exit (8 probes)		
P_{cell}	Cell pressure		
P_f	Fuel pressure at engine manifold	Pressure transducer amplifier, millivolt meter	2% of full scale
P_{h_1}	SF-1 static pressure upstream of metering orifice	Heise gage	0.5 psi
P_{h_2}	SF-1 static pressure downstream of metering orifice	Heise gage	1.0 psi

TABLE I (Continued)

Parameter	Description	Recorder or Indicator	Reading Accuracy
P_{f_1}	Hexane static pressure upstream of metering orifice	Heise gage	0.5 psi
P_{f_2}	Hexane static pressure downstream of metering orifice	Heise gage	2.0 psi
P_{f_t}	Vaporized hexane tank pressure	Heise gage	Not required for data processing
P_{atm}	Atmospheric pressure in blockhouse	Barometer	0.02" Hg
T_{t_o}	Inlet total temperature rake (facility)	Lewis gage	10°F
T_{t_1}	Inlet total temperature downstream of inlet throat	Self-balancing printing potentiometer	2°F
T_{t_2}	Diffuser total temperature upstream of burner	Aspirating Chromel-constantan thermocouple	2°F
T_{w_1}	Combustion chamber wall temperature	Self-balancing printing potentiometer	5°F
T_{w_2}			
T_{w_3}			
T_h	Gaseous fuel temperature at metering venturi	Lewis gage	10°F
T_f	Fuel temperature in engine manifold	Self-balancing printing potentiometer	2°F
T_{f_t}	Hexane temperature in vaporizer tank	Lewis gage	Not required for data reduction
W_f	Liquid fuel flow rate	Rotor-type flow meter-converter	2% of full scale

TABLE II

SUMMARY OF TEST CONFIGURATIONS AND TEST CONDITIONS

Run No.	Tailpipe Length inches	Gutter Type	Orifice Type inches	Number of Fuel Orifices	Combustor Pressure Range psia	Combustor Inlet Temperature °F	Fuel	Equivalence Ratio Range	Remarks
1	60	Short	0.011	80	--	700	Pentaborane	--	No data - fuel manifold immediately clogged - engine started easily with choked exit nozzle.
2	60	Short	0.011	80	2.92 to 3.26	650 to 700	HiCal-3	0.133 to 0.252	Initial data with unclogged fuel system - latter portion of run had 75 percent of injectors clogged. Easily ignited with unchoked exit nozzle.
3	126	Short	0.011	80	2.76 to 3.00	650 to 700	HiCal-3	0.131 to 0.228	75 percent of fuel nozzles clogged early in run.
4	27	Short	0.060	80	2.92 to 3.39	560 to 660	SF-1	0.189 to 0.340	Engine ignition with unchoked exit nozzle.
5	60	Short	0.060	80	3.00 to 3.27	500 to 510	SF-1	0.185 to 0.315	Engine ignition with unchoked exit nozzle.

TABLE II (Continued)

Run No.	Tailpipe Length inches	Gutter Type	Orifice Type inches	Number of Fuel Orifices	Combustor Pressure Range psia	Combustor Inlet Temperature °F	Fuel	Equivalence Ratio Range	Remarks
6	60 nonmetallic tailpipe	Short	0.060	64	3.30 to 3.44	400	SF-1	0.178 to 0.202	Postrun inspection revealed missing fuel nozzle caused hot spot and damage to tailpipe.
7	60 modified nonmetallic tailpipe	Short	0.060	64	3.48 to 3.90	400	SF-1	0.182 to 0.274	Tailpipe modified. Tailpipe still serviceable after 2-1/2 hrs total running time. Only partial delamination of inner combustor surface.
8	60	Extended	0.060	64	2.60 to 4.00	610 to 690	Vaporized Hexane	0.400 to 0.690	Ignition with unchoked exit nozzle.
9	60	Extended	0.060	32	3.00 to 7.60	620 to 690	Liquid Hexane	0.390 to 1.165	Ignition more difficult than with vaporized hexane.
10	60	Short	0.020	64	2.77 to 3.15	400	Pentaborane	0.058 to 0.177	Fuel system clogging was initially slow but progressed rapidly during latter part of run. Postrun inspection revealed 80 percent of injectors plugged.

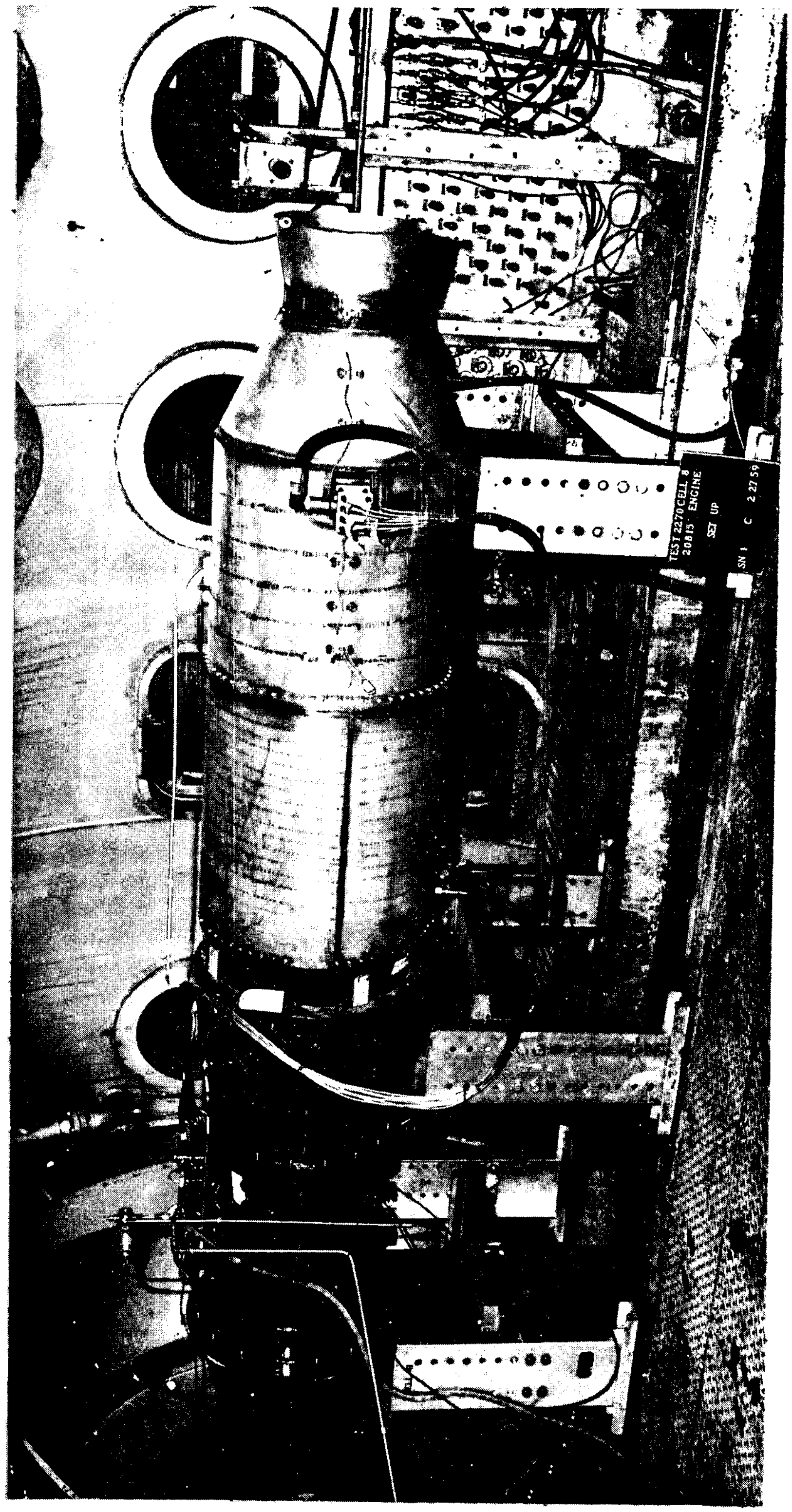

TEST ENGINE INSTALLED IN AF-MJL CELL 8 FACILITY

ENGINE INSTALLATION SCHEMATIC
AF-MJL - CELL 8

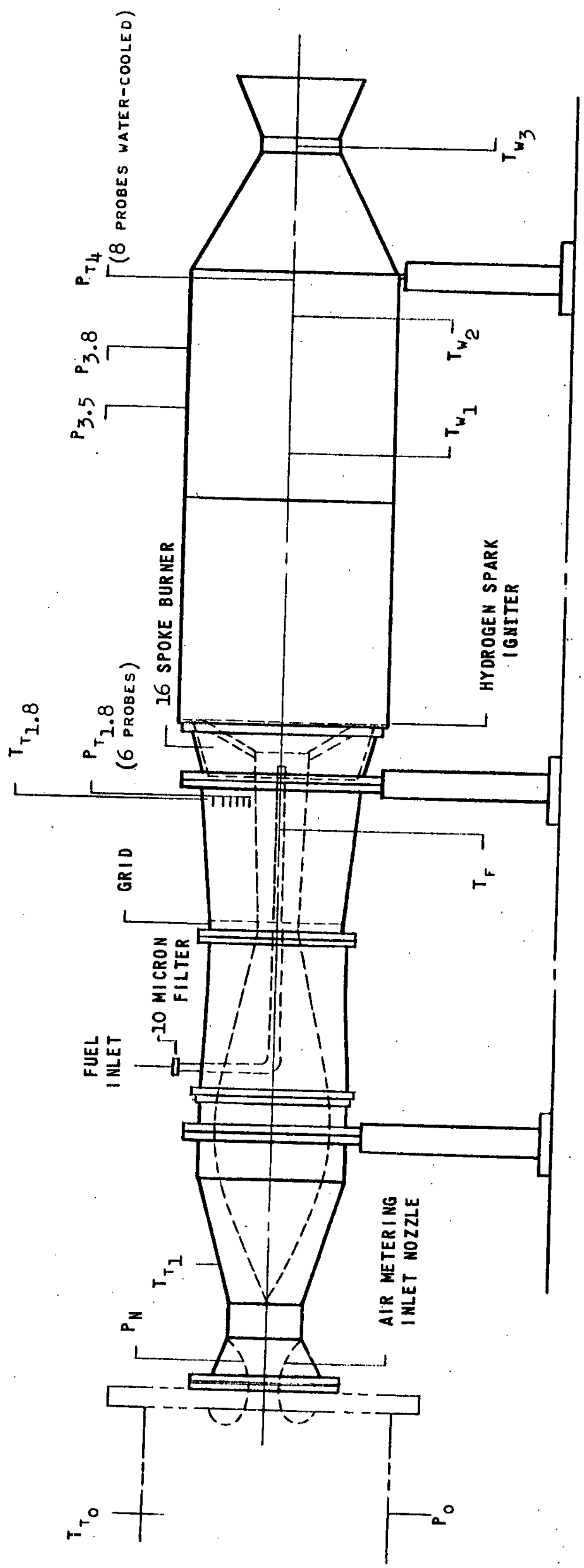

SCHEMATIC OF GUTTER AND INJECTOR CONFIGURATION

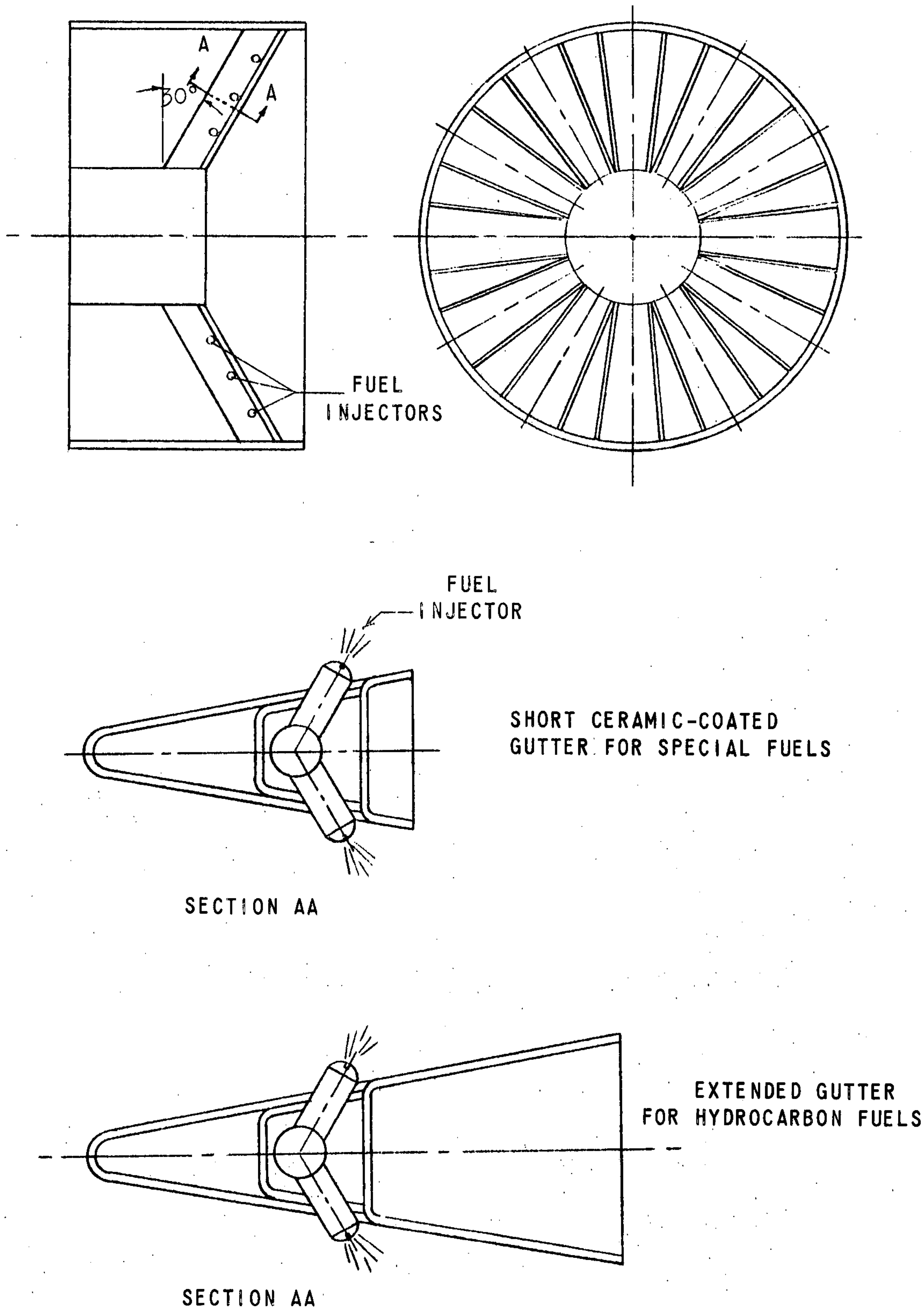

BASIC COMBUSTOR CONFIGURATION
WITH SHORT CERAMIC-COATED GUTTERS

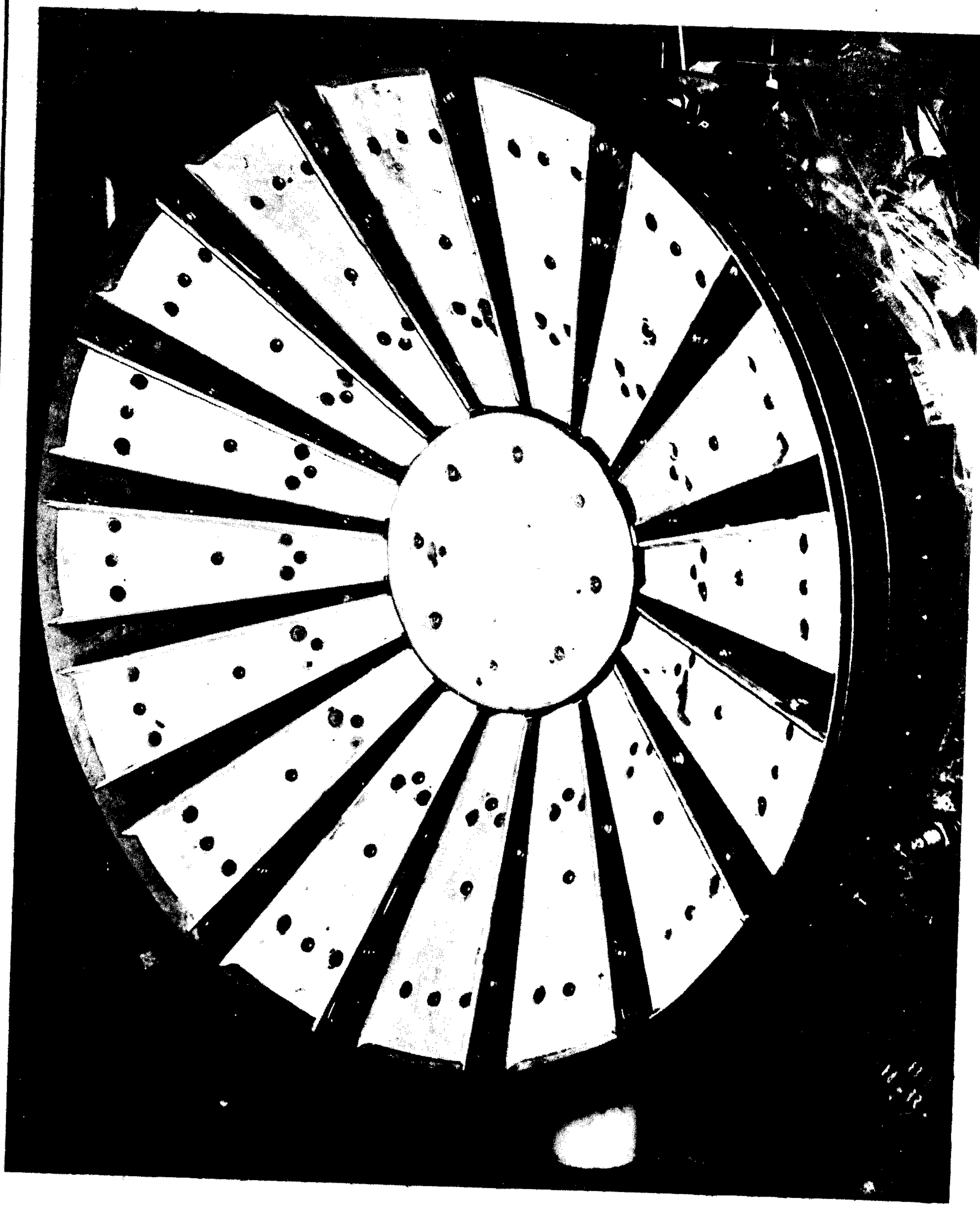

MODIFIED SPOKE-GUTTER COMBUSTOR CONFIGURATION
WITH EXTENDED GUTTERS

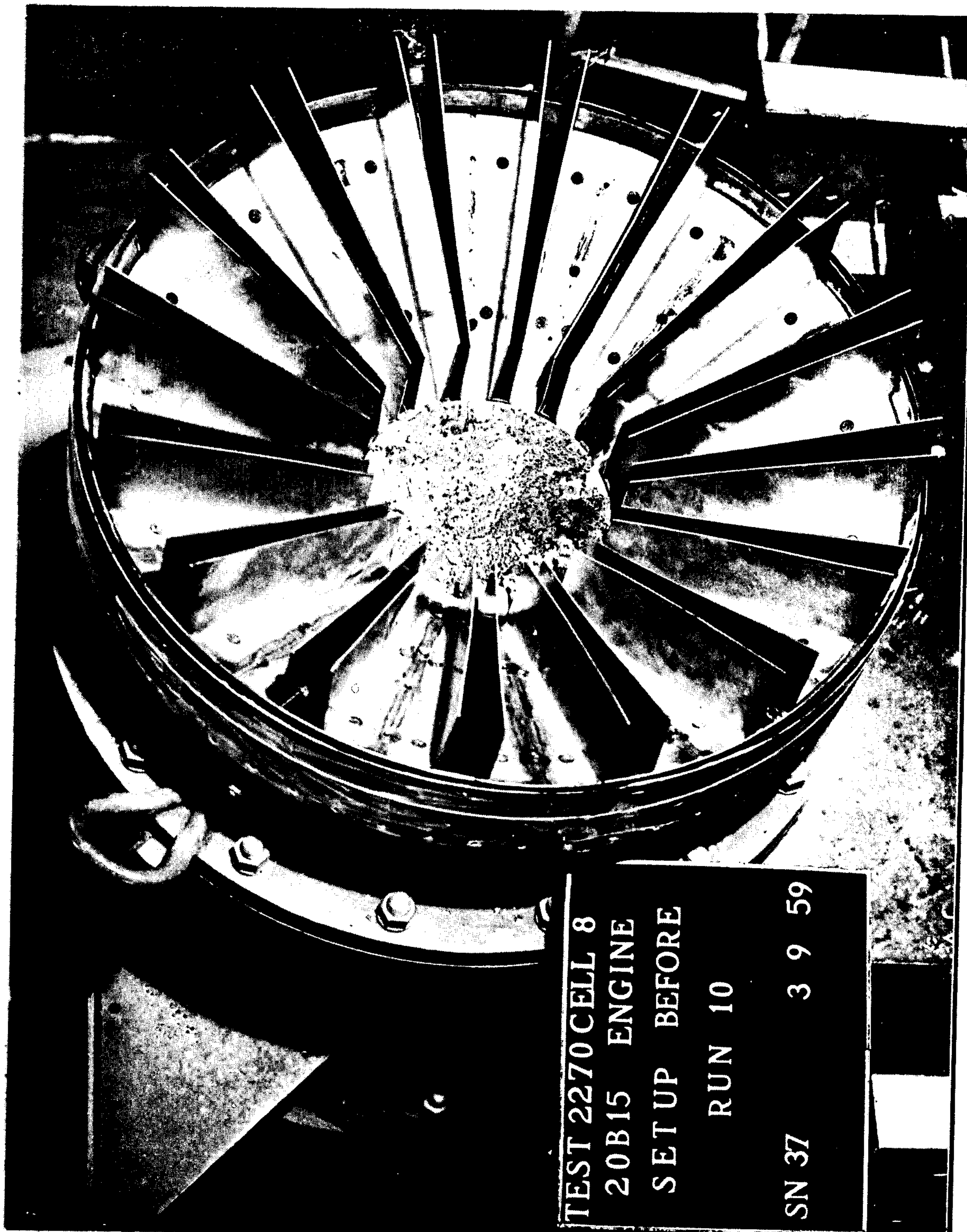

NONMETALLIC TAILPIPE BEFORE INSTALLATION

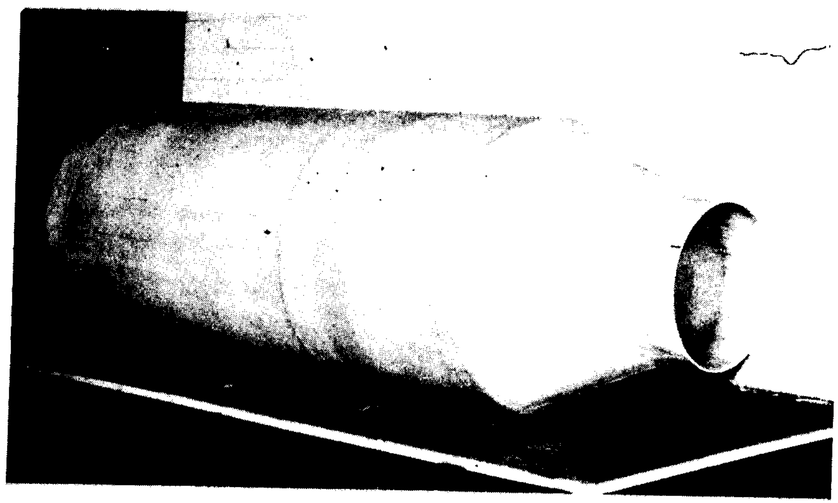

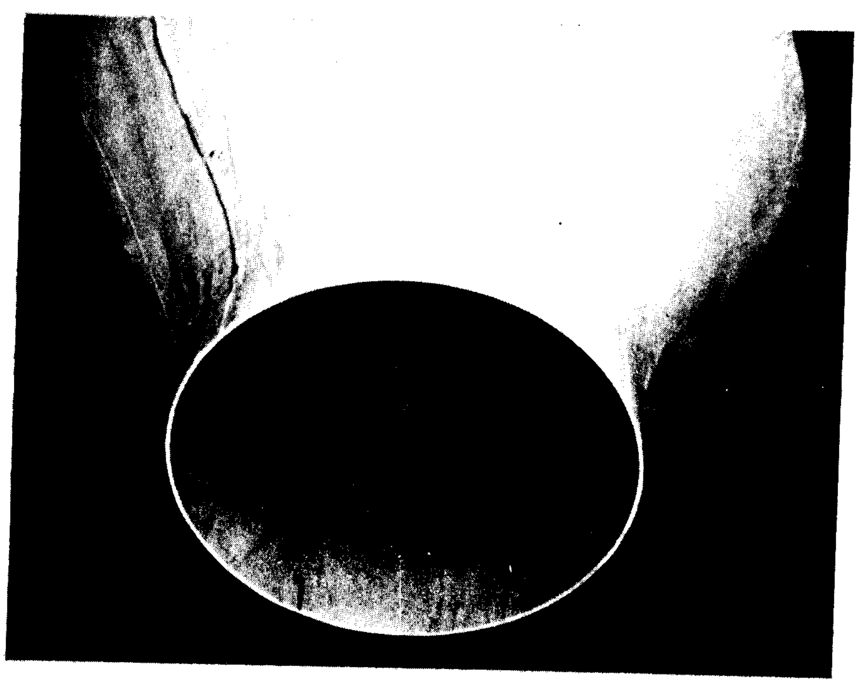

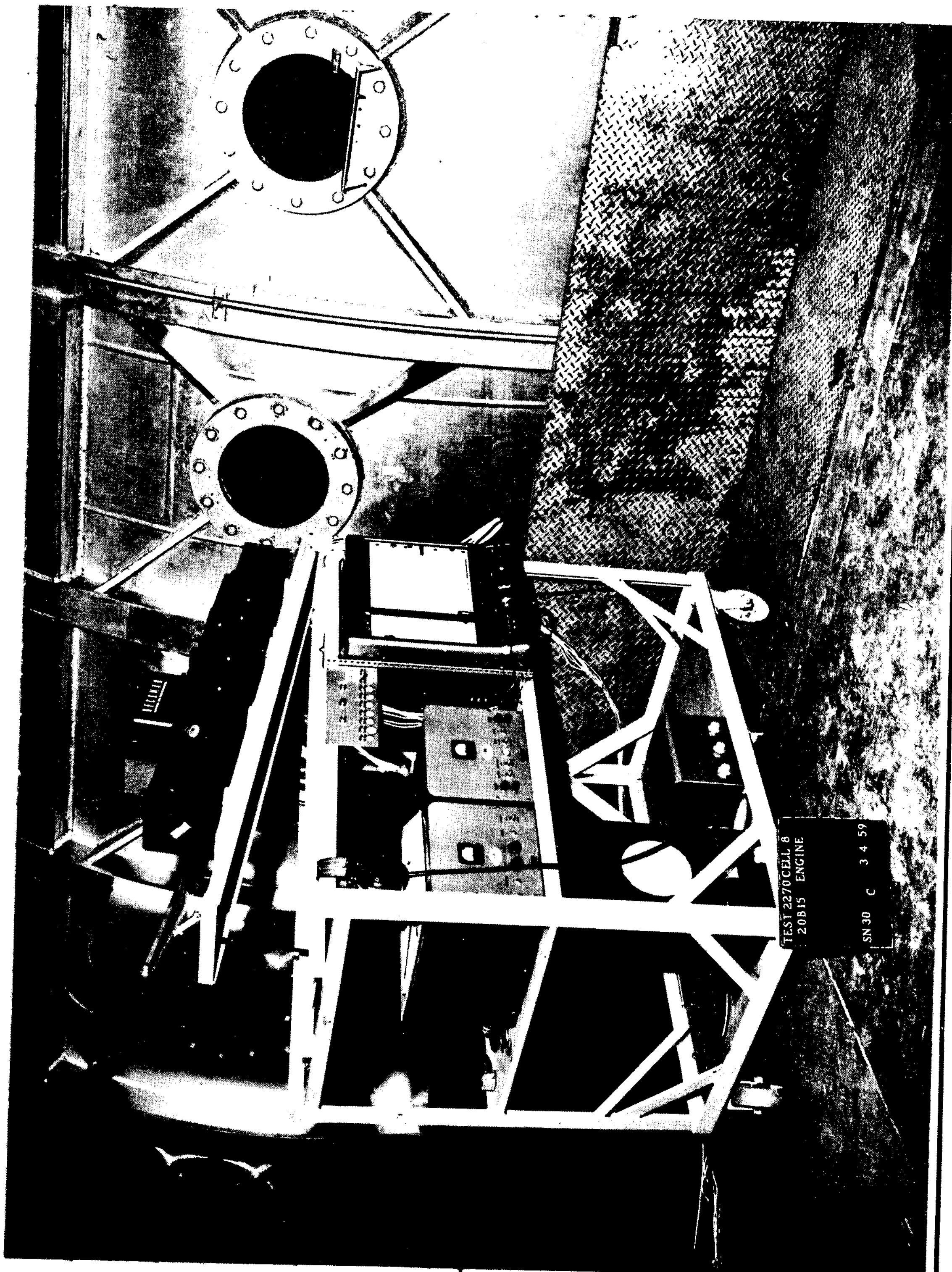

INSTALLATION OF INFRARED SPECTROMETER AND ASSOCIATED EQUIPMENT

COMBUSTION EFFICIENCY SUMMARY CURVES

HiCAL-3, PENTABORANE, SF-1, LIQUID HEXANE, AND VAPORIZED HEXANE

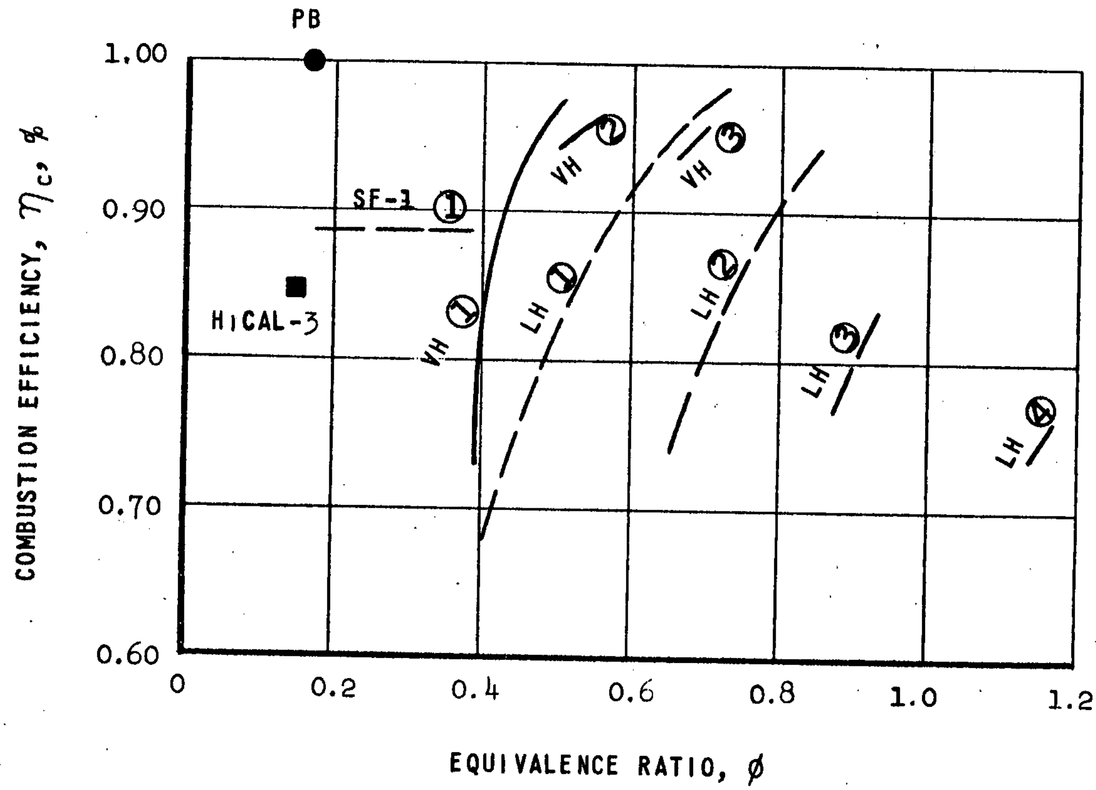

LEGEND			
CURVE	FUEL	ALTITUDE THOUSAND FT	M_0
■	HiCAL-3	100	3.0
SF-1 ①	SF-1	98	2.6-2.7
VH ①	VAPORIZED HEXANE	98	3.0
VH ②		102	3.0
VH ③		106	2.9
LH ①	LIQUID HEXANE	87	3.1
LH ②		100	2.85
LH ③		103	2.8
LH ④		106	2.8
● PB	PENTABORANE	98-103	2.3-2.5

SECRET

FIGURE 8

COMBUSTION PERFORMANCE OF SF-1

RUNS 4 AND 5

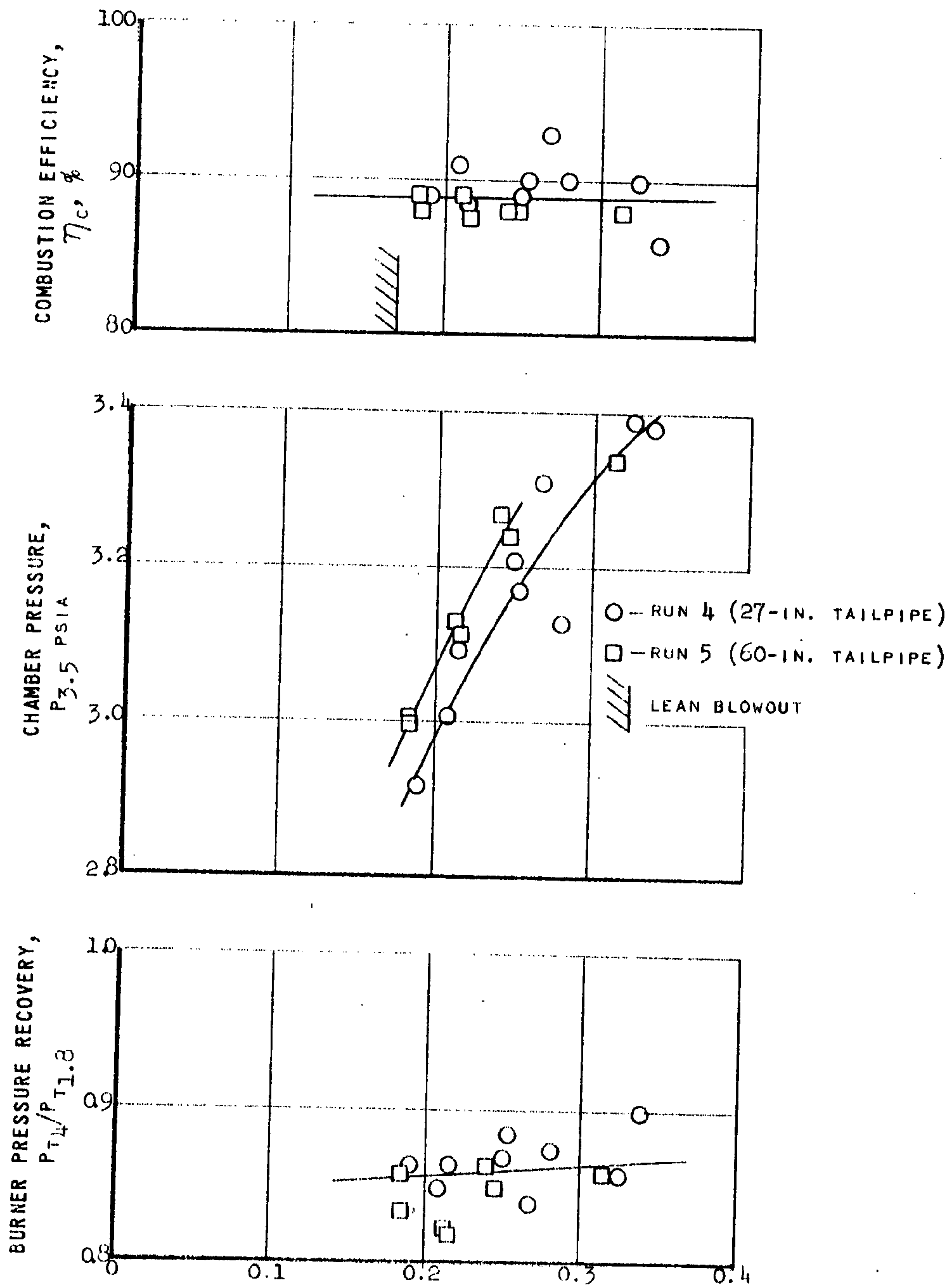

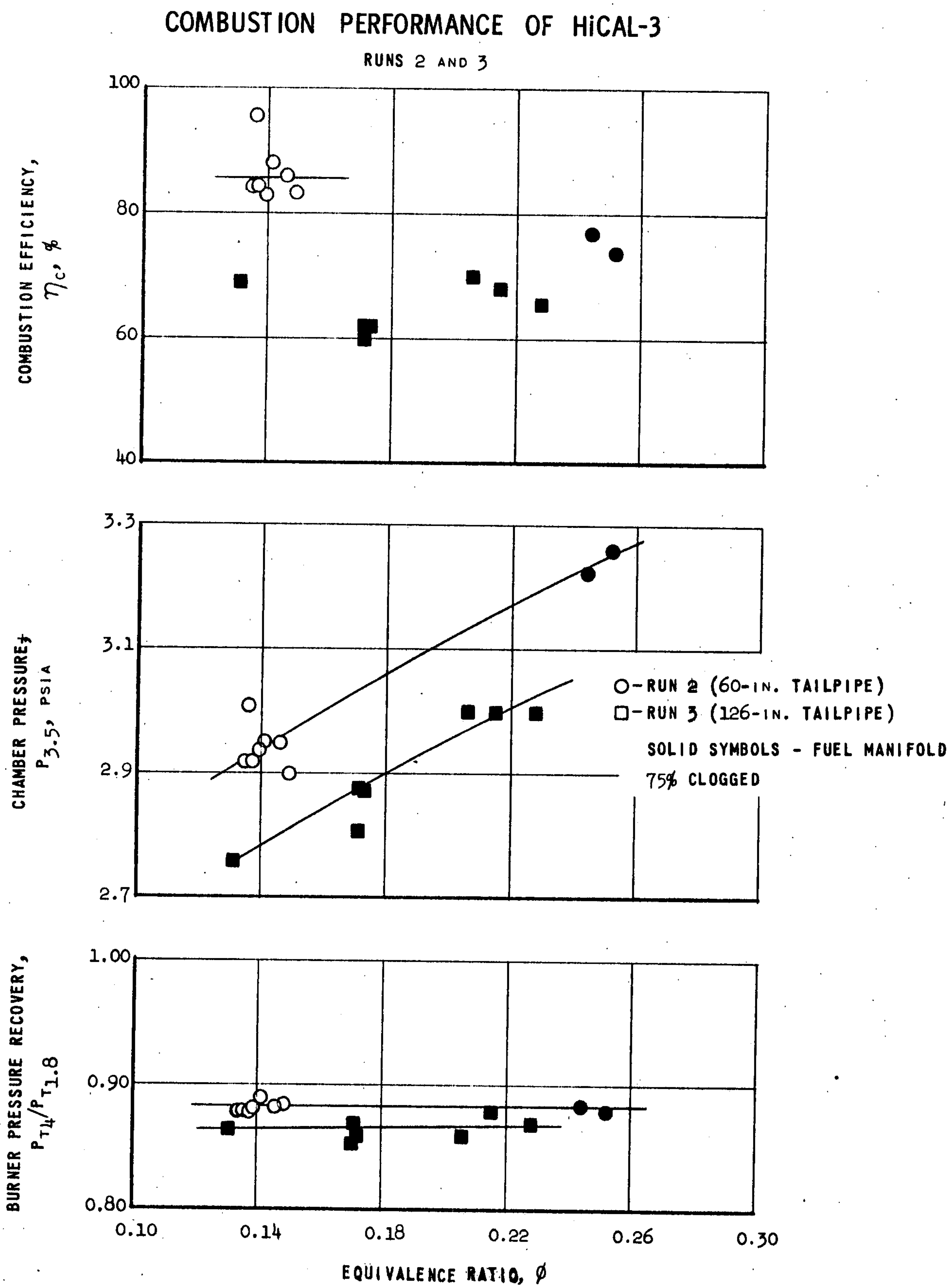
COMBUSTION PERFORMANCE OF HiCAL-3
RUNS 2 AND 3
COMBUSTION EFFICIENCY, η_c, %
100
80
60
40
CHAMBER PRESSURE, $P_{3.5}$, PSIA
3.3
3.1
2.9
2.7
O-RUN 2 (60-IN. TAILPIPE)
□-RUN 3 (126-IN. TAILPIPE)
SOLID SYMBOLS - FUEL MANIFOLD 75% CLOGGED
BURNER PRESSURE RECOVERY, $P_{T4}/P_{T1.8}$
1.00
0.90
0.80
0.10
0.14
0.18
0.22
0.26
0.30
EQUIVALENCE RATIO, ϕ

SOLID DEPOSITS ON CLOGGED FACILITY AND ENGINE FILTERS AFTER RUN 2 -- PENTABORANE FUEL

CLOGGED FUEL MANIFOLDS WITH FILTERS REMOVED AFTER RUN 2 -- PENTABORANE FUEL

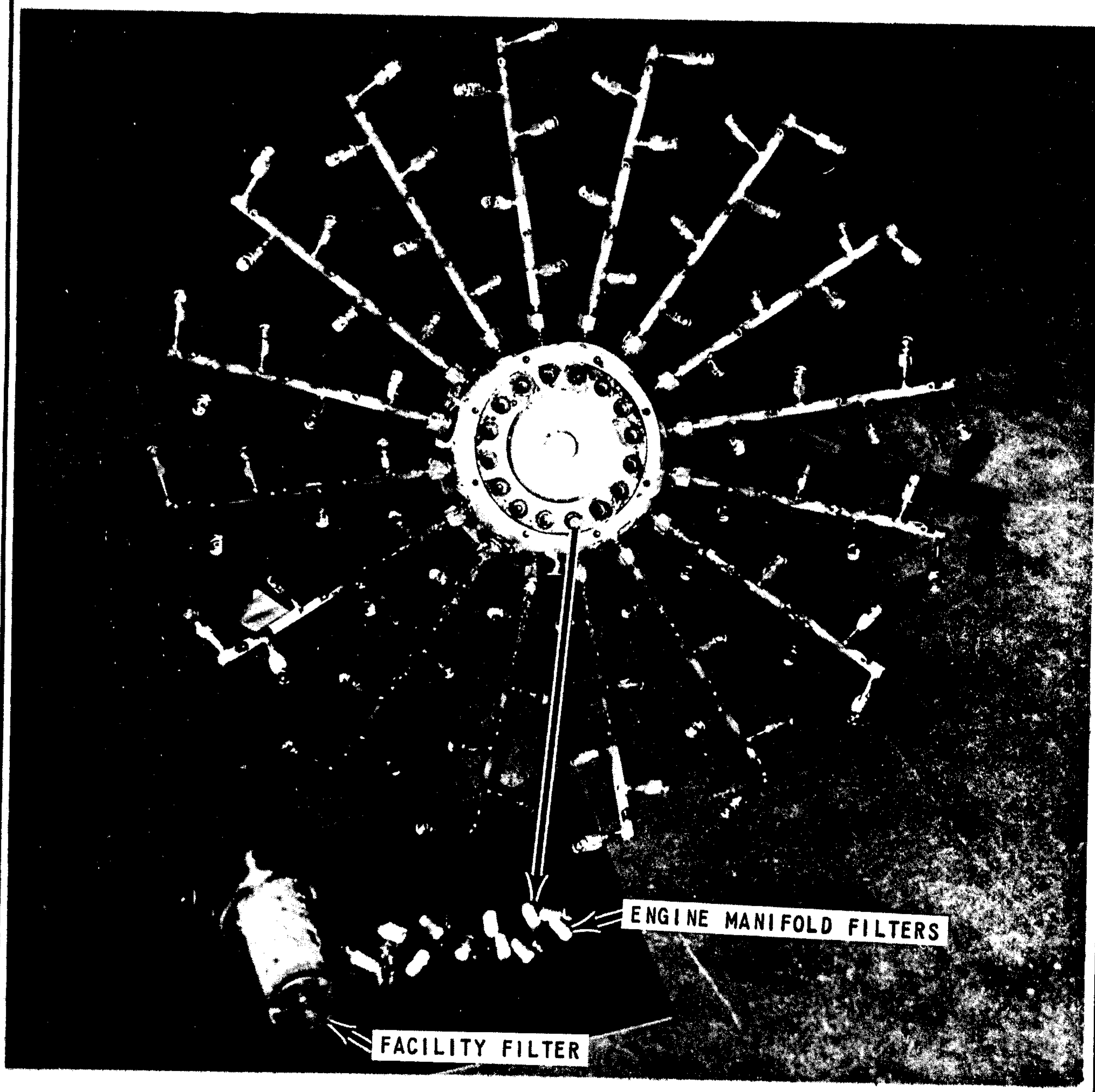

COMBUSTION PERFORMANCE OF PENTABORANE

RUN 10

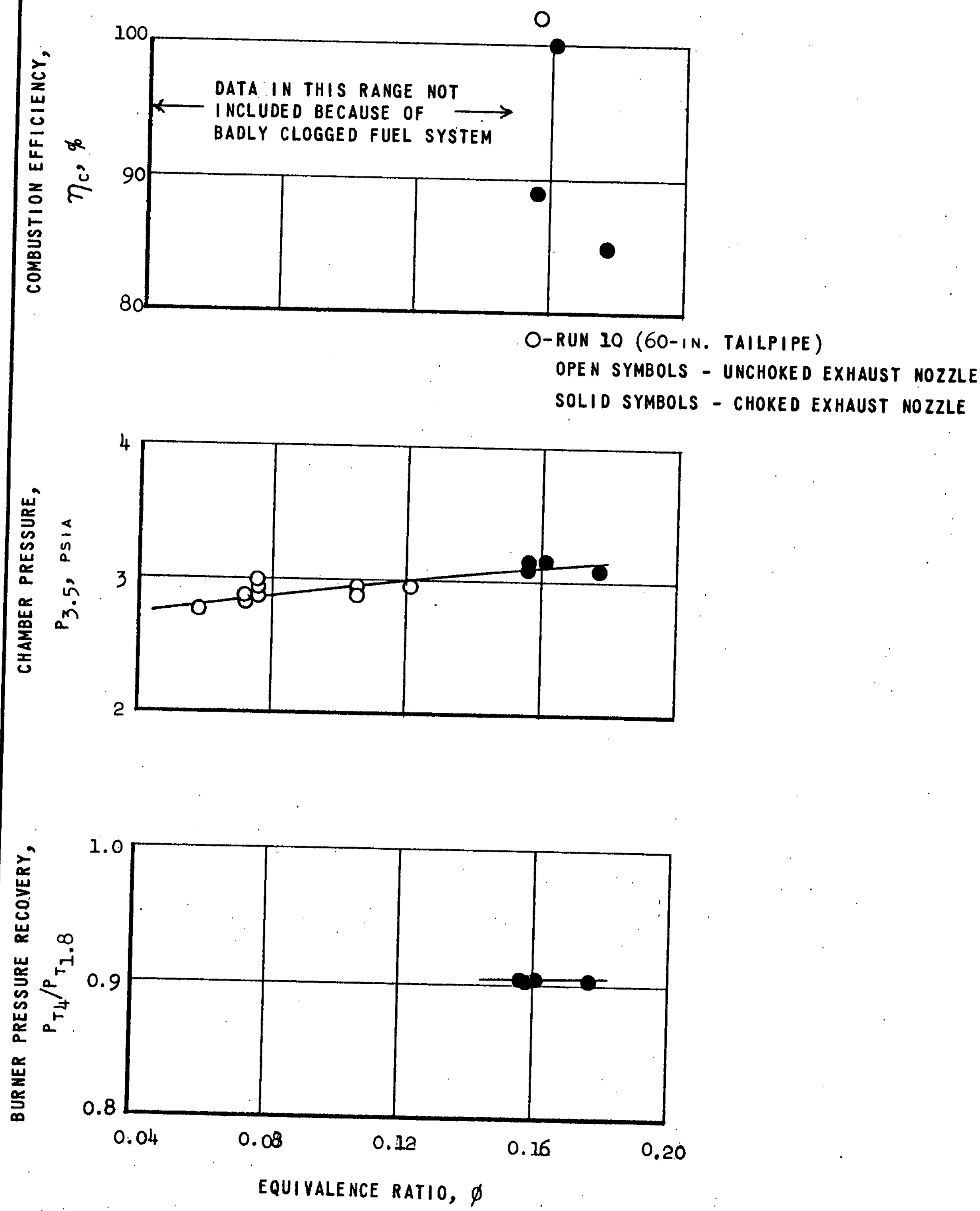

COMBUSTION PERFORMANCE OF VAPORIZED HEXANE

RUN 8

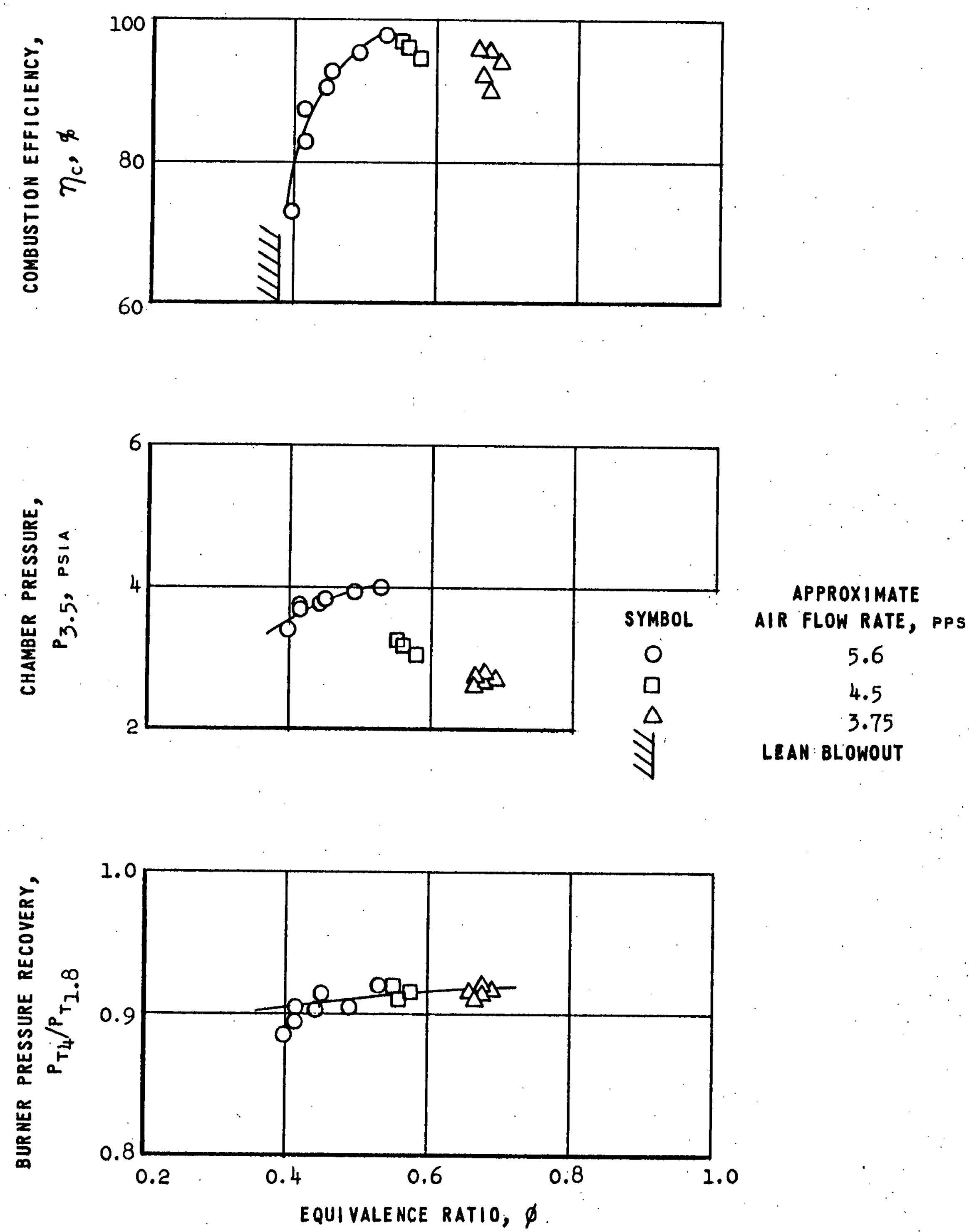

Declassified in Part - Sanitized Copy Approved for Release 2012/08/14 : CIA-RDP89B00487R000400750006-4

COMBUSTION PERFORMANCE OF LIQUID HEXANE

RUN 9

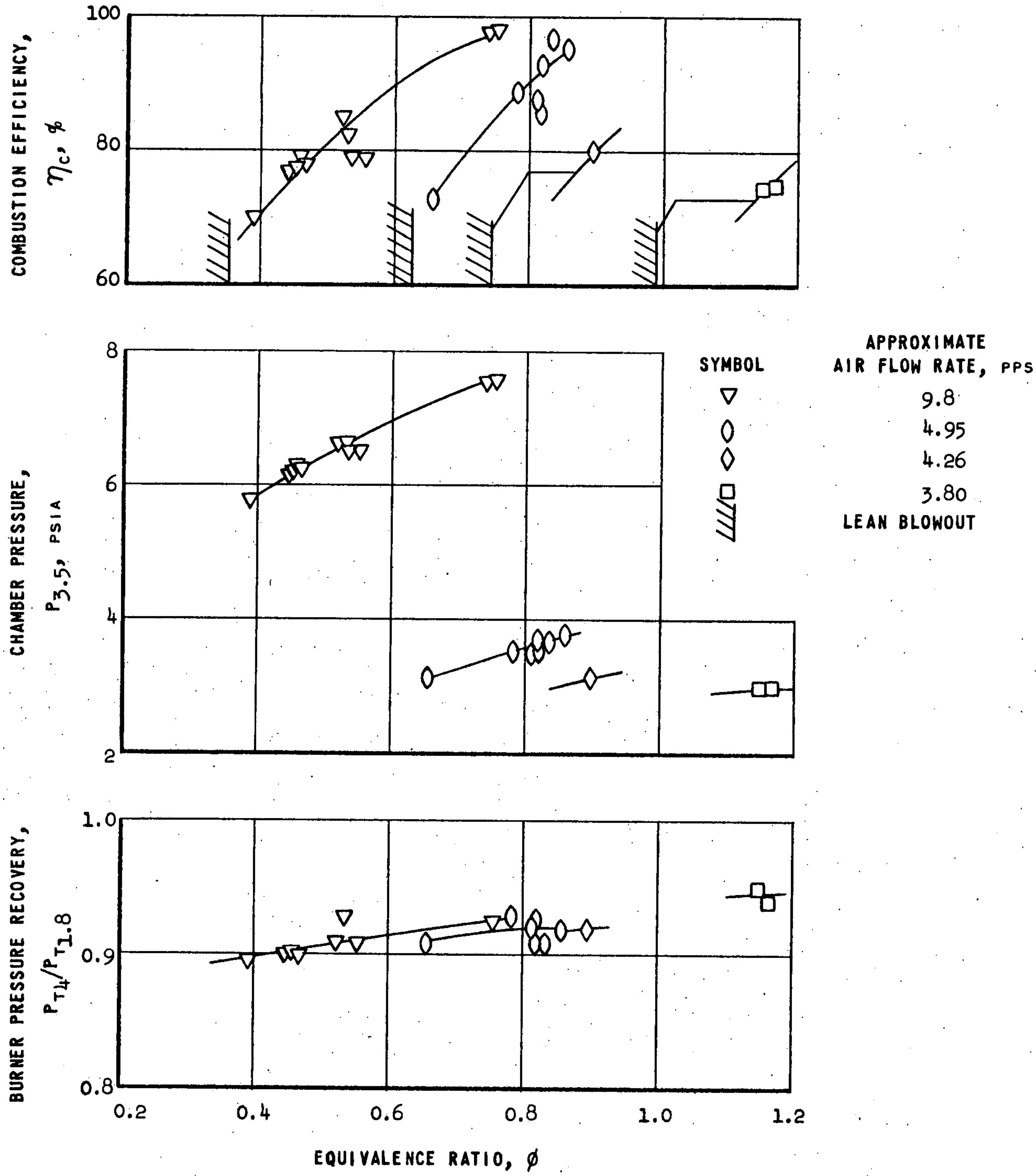

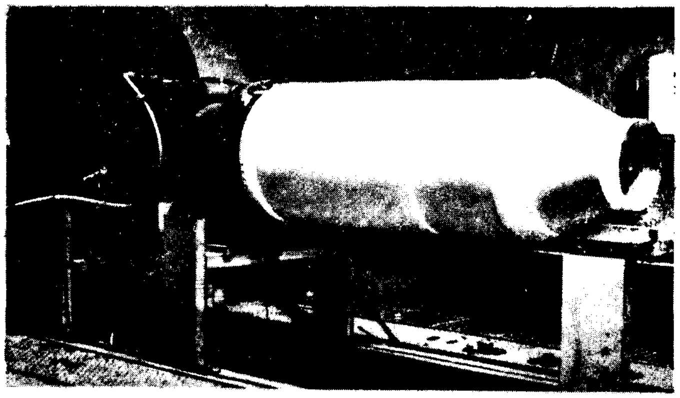

A. NONMETALLIC TAILPIPE

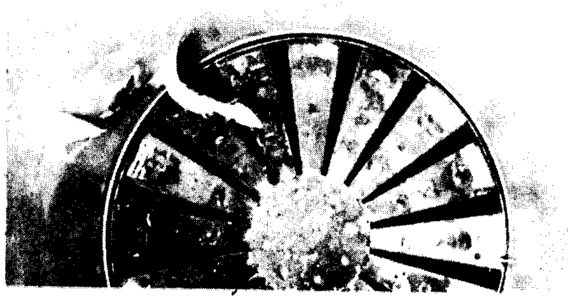

B. LOCALIZED DAMAGE TO NONMETALLIC TAILPIPE RESULTING FROM FUEL NOZZLE MALFUNCTION

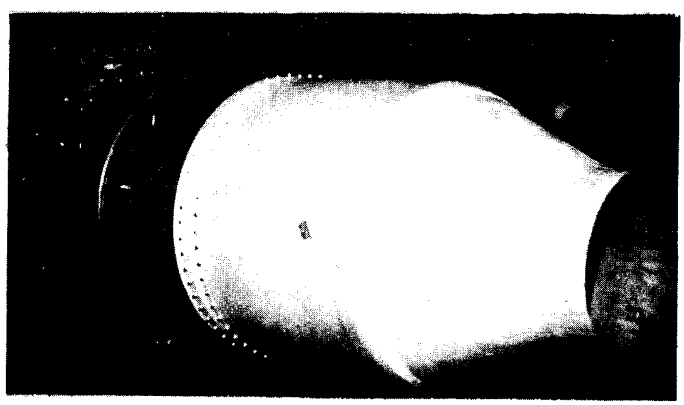

C. REWORKED NONMETALLIC TAILPIPE

TIME HISTORIES ON NONMETALLIC TAILPIPE ENDURANCE TEST

RUN 6

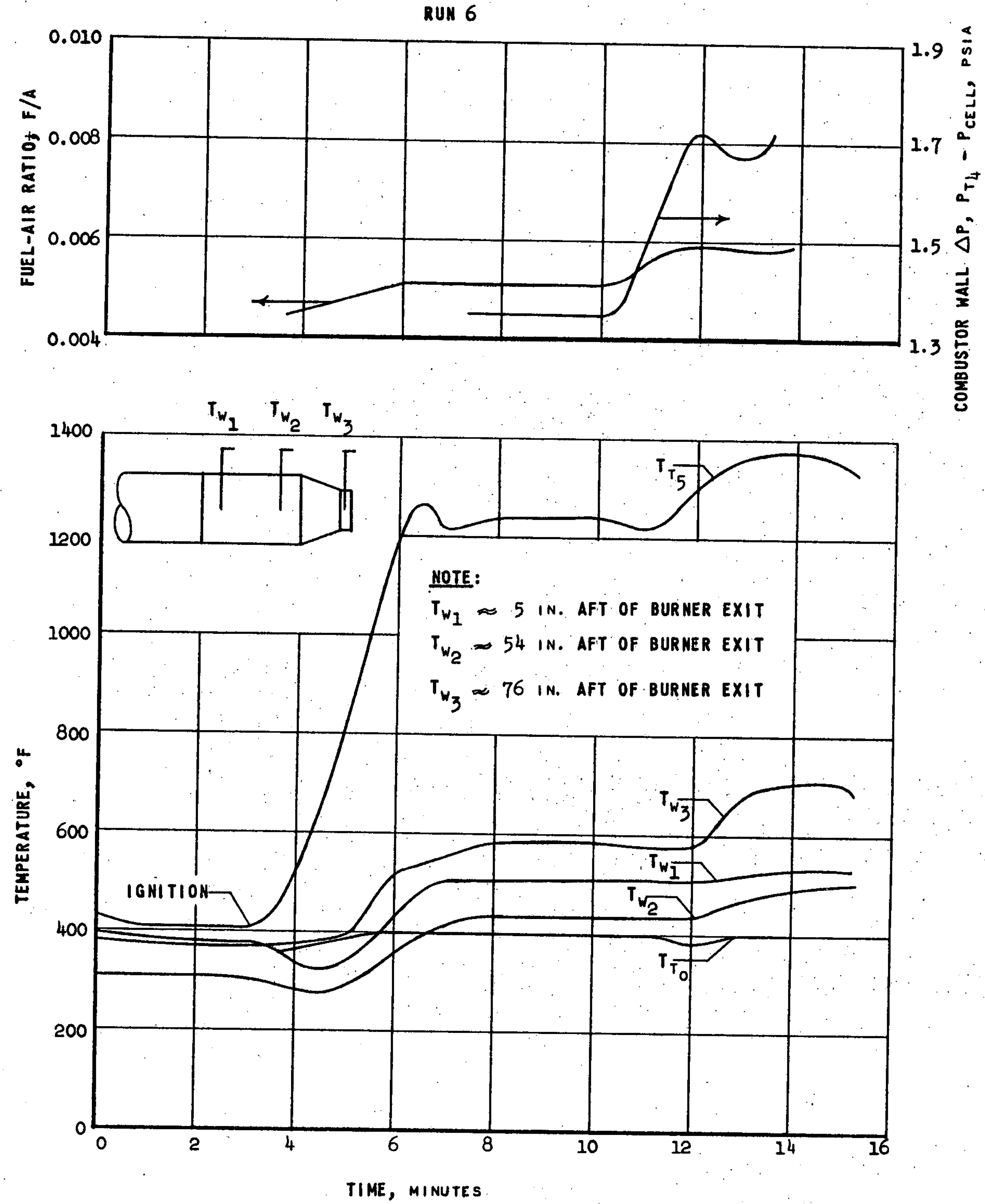

TIME HISTORIES OF NONMETALLIC TAILPIPE ENDURANCE TEST

RUN 7

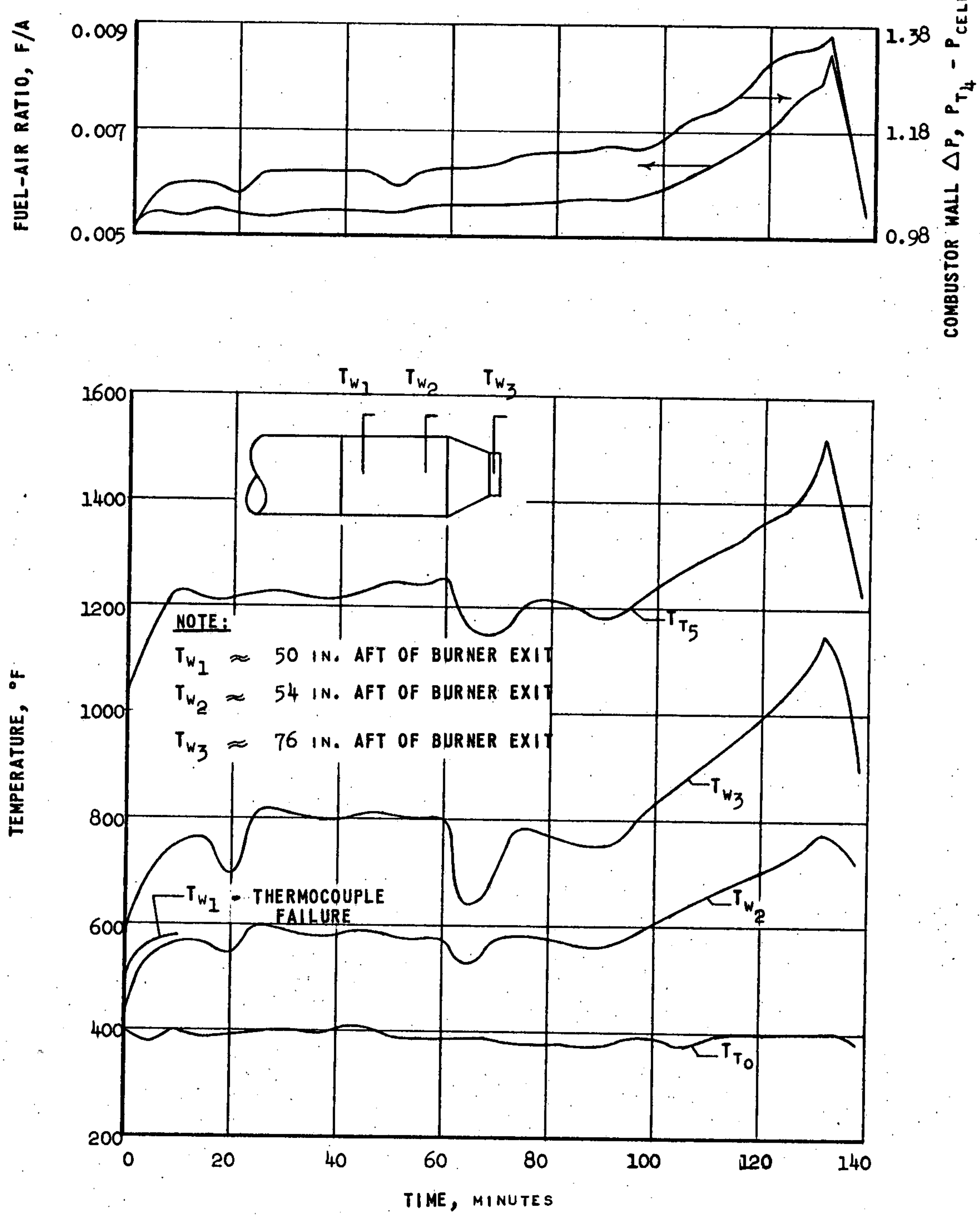

PARTIAL DELAMINATION OF NONMETALLIC TAILPIPE
AFTER 2 1/2 HOURS BURNING TIME

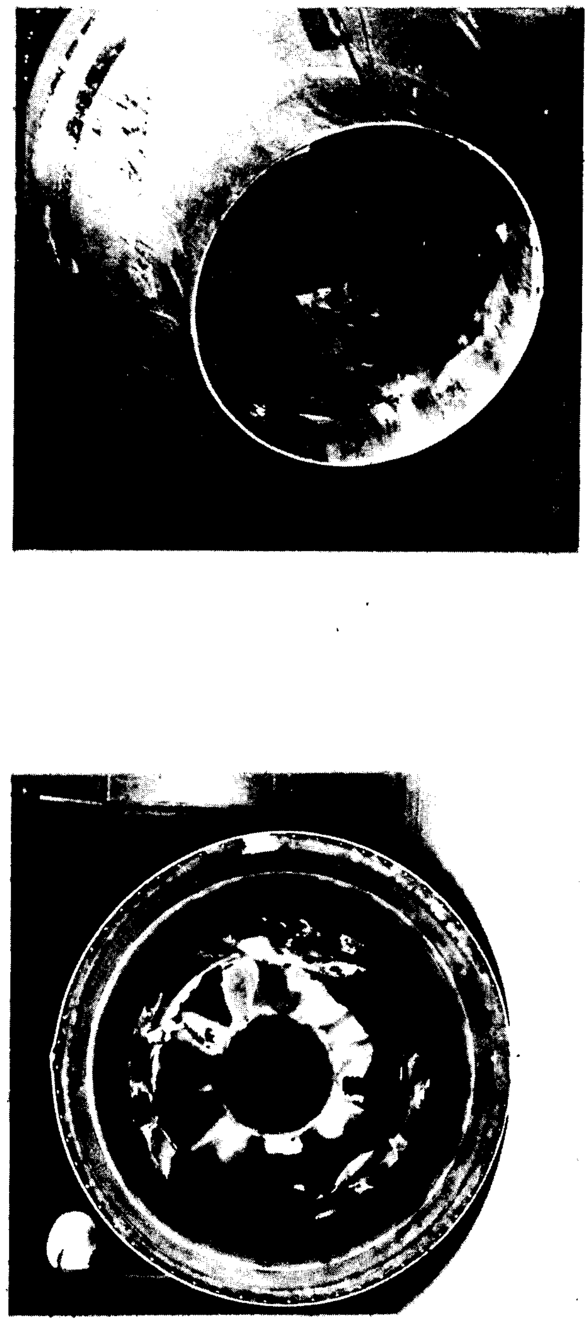

INFRARED RADIANT EMITTANCE OF SEVERAL FUELS

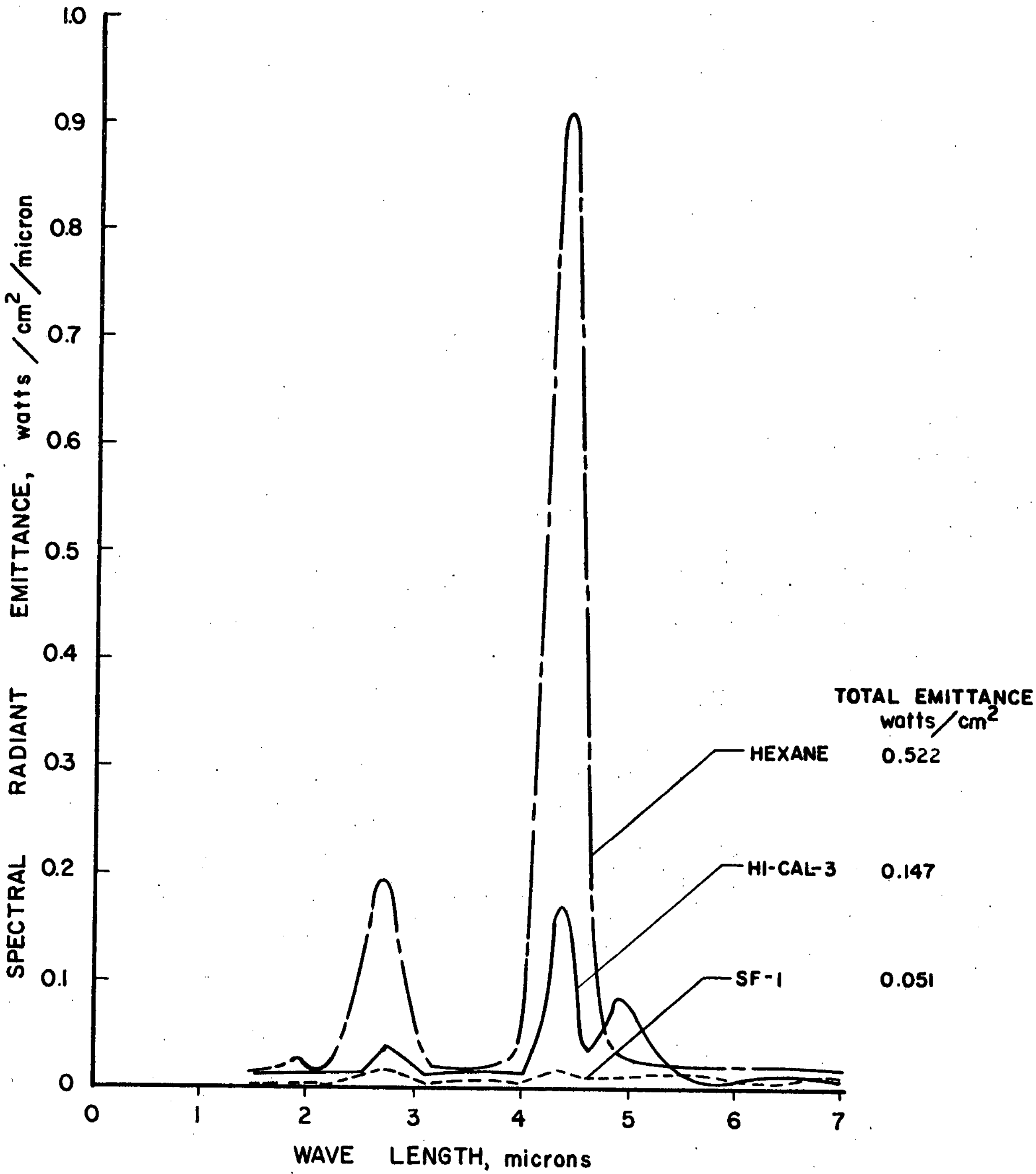

ASSUMED COMBUSTION EFFICIENCY VARIATION FOR OPTIMIZATION STUDY

PENTABORANE FUEL

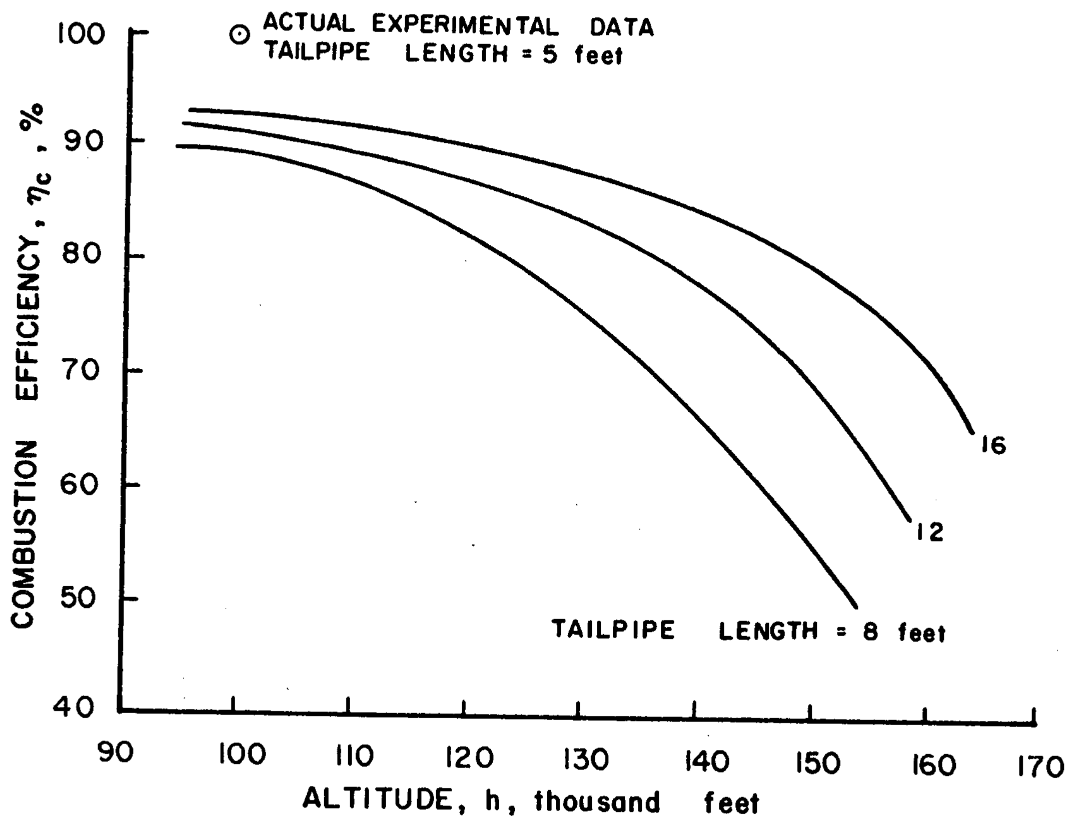

IDEAL COMBUSTION TEMPERATURE RISE vs FUEL-AIR RATIO FOR PENTABORANE

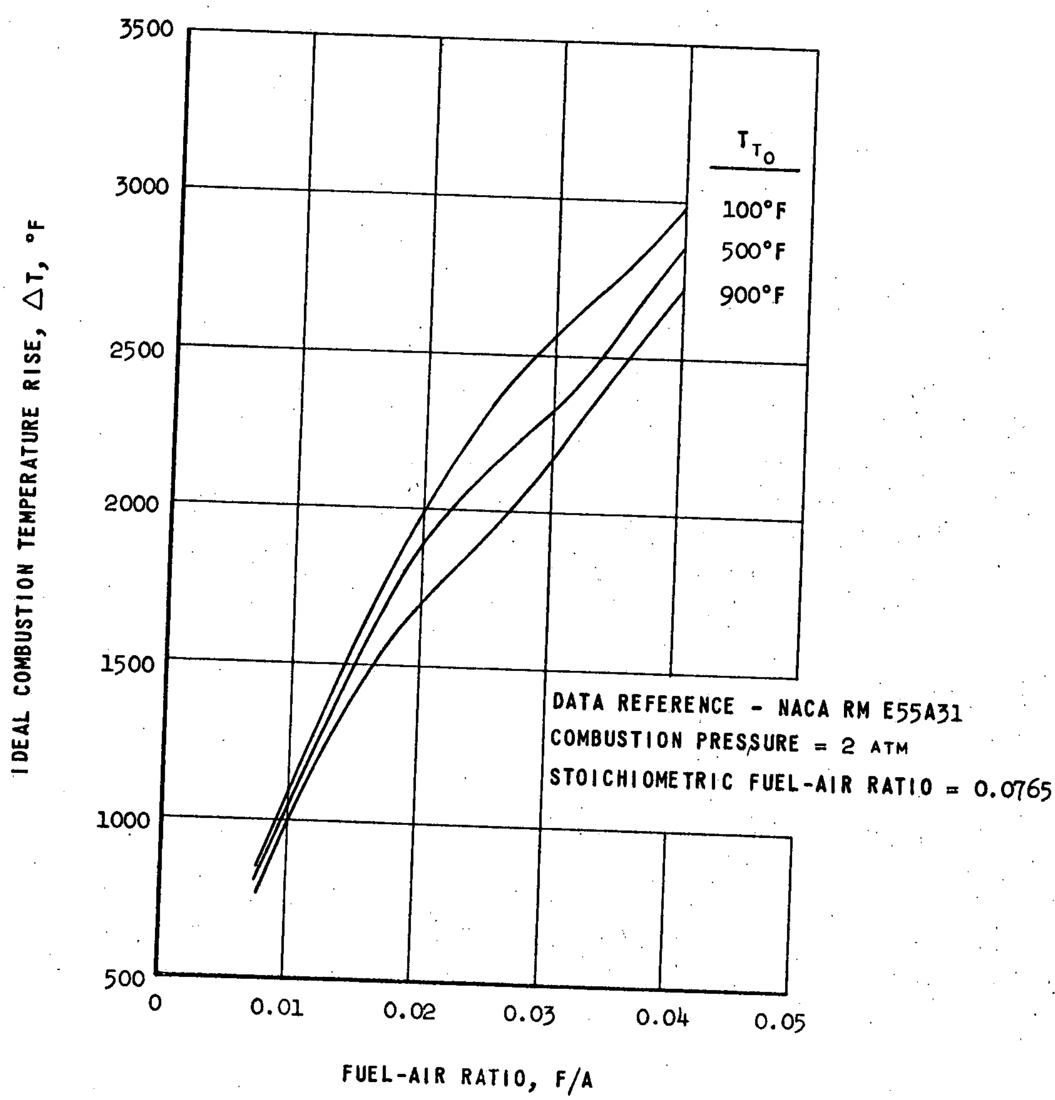

IDEAL COMBUSTION TEMPERATURE RISE vs FUEL-AIR RATIO FOR PENTABORANE, HiCAL-3, AND HEXANE

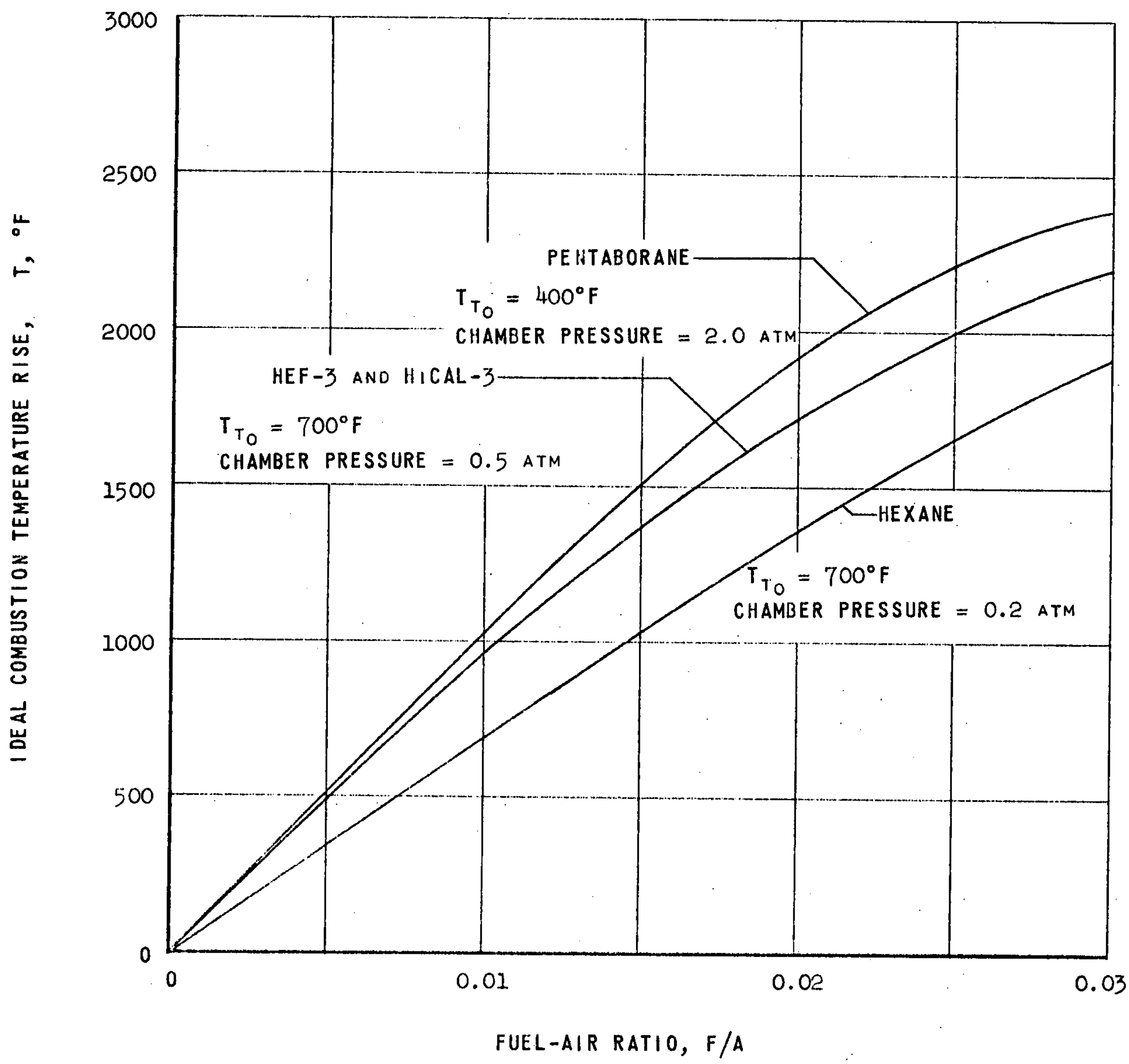

IDEAL COMBUSTION TEMPERATURE RISE vs FUEL-AIR RATIO FOR SF-1

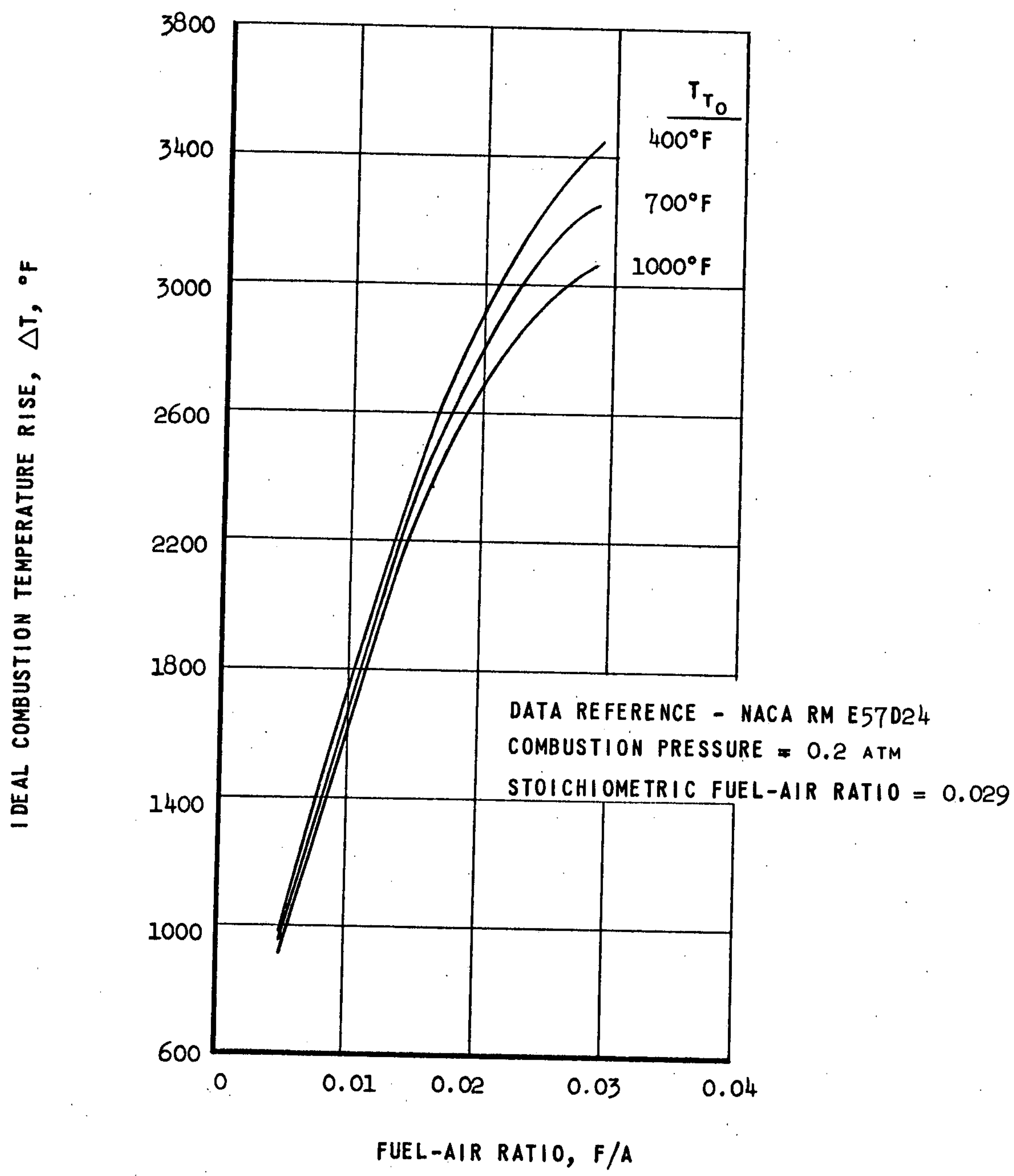

THERMODYNAMIC PROPERTIES OF SF-1 AND AIR COMBUSTION PRODUCTS

NO DISSOCIATION
INLET TEMPERATURE = 700°F